



# Calcium isotope evidence for dramatic increase of continental weathering during the Toarcian oceanic anoxic event (Early Jurassic)



Jean-Michel Brazier<sup>a</sup>, Guillaume Suan<sup>a,\*</sup>, Théo Tacail<sup>b</sup>, Laurent Simon<sup>c</sup>, Jeremy E. Martin<sup>a</sup>, Emanuela Mattioli<sup>a</sup>, Vincent Balter<sup>b</sup>

<sup>a</sup> UMR CNRS 5276 LGLTPE, Université Claude Bernard Lyon 1, Ecole Normale Supérieure de Lyon, Bâtiment Géode, F-69622 Villeurbanne Cedex, France

<sup>b</sup> UMR CNRS 5276 LGLTPE, Université Claude Bernard Lyon 1, Ecole Normale Supérieure de Lyon, 46 Allée d'Italie, F-69364 Lyon Cedex 07, France

<sup>c</sup> UMR CNRS 5023 LEHNA, Université Claude Bernard Lyon 1, Bâtiment Forel, F-69622 Villeurbanne Cedex, France

## ARTICLE INFO

### Article history:

Received 18 March 2014

Received in revised form 6 November 2014

Accepted 21 November 2014

Available online xxxx

Editor: J. Lynch-Stieglitz

### Keywords:

calcium isotopes

Pliensbachian–Toarcian

Karoo–Ferrar

continental weathering

oceanic anoxic event

## ABSTRACT

The early Toarcian was punctuated by pulses of massive carbon injection that are thought to have triggered, through increased greenhouse conditions, elevated continental discharge and nutrient input, marine anoxia, seawater acidification and species extinctions. Nevertheless, the mode and tempo of changes in continental weathering across this interval remains highly debated, leading to considerable uncertainty about the main causes of these perturbations. In this study we present calcium isotope measurements ( $\delta^{44/40}\text{Ca}$ ) of well-preserved brachiopods and bulk rock samples from the hemipelagic strata of Pliensbachian–Toarcian age of Peniche in Portugal in order to constrain changes in the calcium cycle and hence changes in continental weathering during the early Toarcian. The data reveal a similar trend as carbon isotope data from the same section and show negative excursions of about 0.5‰ at the Pliensbachian–Toarcian transition (PI–To) and at the base of the Toarcian Oceanic Anoxic Event (T–OAE) interval. The comparison of  $\delta^{44/40}\text{Ca}$  ratios recorded in brachiopods and bulk rock corrected for variable dolomite contribution indicates that these excursions reflect changes in the global isotopic composition of seawater rather than changes in the dominant mineralogy of calcifying organisms or in hydrological budget of the considered basin. Box modeling results suggest that the PI–To and T–OAE  $\delta^{44/40}\text{Ca}$  excursions can be explained by a transient 90% decrease of carbonate accumulation due to seawater acidification followed by a 500% increase in continental weathering rates. The sharp increases in continental weathering inferred from the  $\delta^{44/40}\text{Ca}$  ratios seem overall consistent with lower Toarcian sedimentological and biotic records that document rapid crises in carbonate production followed by episodes of increased calcium carbonate burial. Nevertheless, the maximum of carbonate burial recorded by most NW European basinal successions occurs several hundreds of kyrs after that predicted by box modeling results. This mismatch either implies that the European records of carbonate accumulation do not reflect global trends or that the fundamental processes related to the removal of excess alkalinity caused by increased continental weathering are more complex than previously appreciated. Based on the amount of Ca input simulated by box modeling, the injection of tens of thousands of gigatons of carbon with an isotopic composition ( $\delta^{13}\text{C}$ ) comprised between  $-6\text{‰}$  and  $-14\text{‰}$  appears as the most likely causes of the  $\delta^{13}\text{C}$  excursions characterizing these two events. These results indicate that environmental and biotic changes of the PI–To and T–OAE were mainly caused a cascade of environmental changes triggered by the massive carbon emissions from the Karoo–Ferrar volcanism.

© 2014 Elsevier B.V. All rights reserved.

## 1. Introduction

The lower Toarcian (Lower Jurassic, 183 Ma ago) deposits record some of the most severe environmental perturbations of the Mesozoic. This time interval was punctuated by second-order global

extinction or severe assemblage changes affecting pelagic and benthic organisms (Palliani and Riding, 2003; Cecca and Macchioni, 2004; Gómez et al., 2008; Wignall and Bond, 2008; Mattioli et al., 2009), especially at the Pliensbachian–Toarcian boundary (PI–To) and in the latest *tenuicostatum* ammonite Zone, broadly coinciding with the onset of the Toarcian oceanic anoxic event (T–OAE). The lower Toarcian interval is also characterized by common black shale deposits that are thought to reflect the widespread

\* Corresponding author.

E-mail address: guillaume.suan@univ-lyon1.fr (G. Suan).

development of poor oxygenation in the oceans (Jenkyns, 1988, 2010). Generalized carbonate production crisis also took place during these two events and were characterized by a drastic size reduction of the main pelagic carbonate producer *Schizosphaerella* (Mattioli and Pittet, 2002; Suan et al., 2008a), near disappearance of shallow-water platforms (Dromart et al., 1996; Trecalli et al., 2012) and decrease in carbonate accumulation in basinal succession (Mattioli et al., 2004, 2009).

Importantly, marine carbonates and organic carbon from several sites around the world record pronounced ( $\sim 2\text{--}5\%$ ) negative carbon isotope excursions (CIE) at the PI-To and T-OAE (Hesselbo et al., 2000; Jenkyns et al., 2001; Kemp et al., 2005; Hesselbo et al., 2007; Littler et al., 2010; Al-Suwaidi et al., 2010; Caruthers et al., 2011; Suan et al., 2011; Izumi et al., 2012). The duration of the T-OAE negative CIE has been suggested to be in the order of  $\sim 300$  to  $900$  kyr (Kemp et al., 2005; Suan et al., 2008b; Huang and Hesselbo, 2013; Boulila et al., 2014). Recent spectral analyses of expanded sections in Morocco suggest slightly lower duration for the PI-To event ( $\sim 400$  kyrs; Krencker et al., 2013). These negative CIEs, first interpreted as consequences of diagenetic processes or regional upwellings of  $^{13}\text{C}$ -depleted water masses (Küspert, 1982; Jenkyns, 1988), have been also evidenced in fossil wood (Hesselbo et al., 2000, 2007; Al-Suwaidi et al., 2010; Caruthers et al., 2011), suggesting a substantial input of  $^{13}\text{C}$ -depleted carbon into the atmosphere–ocean system.

Two main hypotheses have been proposed to explain these pulses of  $^{13}\text{C}$ -depleted carbon release, namely, methane hydrate dissociation from marine sediments ( $\delta^{13}\text{C} \sim -60\%$ ) and thermogenic methane emissions from Karoo–Ferrar large igneous province (LIP) ( $\delta^{13}\text{C} \sim -40\%$ ) (Hesselbo et al., 2000; Kemp et al., 2005; McElwain et al., 2005; Svensen et al., 2007). An episode of substantial carbon input during the T-OAE is supported by the marked seawater temperature rise ( $\sim 4\text{--}7^\circ\text{C}$ ) inferred from  $\delta^{18}\text{O}$  of brachiopods shells from Peniche section (Portugal) (Suan et al., 2008a, 2010) and belemnite Mg/Ca and  $\delta^{18}\text{O}$  ratios from various European sections (McArthur et al., 2000; Bailey et al., 2003). A marked increase in seawater temperatures at the onset of the PI-To has been also deduced from brachiopod  $\delta^{18}\text{O}$  ratios (Suan et al., 2008a). These pulses of massive carbon input are thought to have triggered a carbonate system crisis through higher  $\text{CO}_2$  levels and associated change in ocean chemistry (ocean acidification; Suan et al., 2008a; Trecalli et al., 2012). Besides, higher global temperatures may have led to accelerated hydrological cycle, continental chemical weathering and nutrient input to the oceanic reservoir (Cohen et al., 2004; Jenkyns, 2010). These conditions likely favored higher primary organic productivity and organic matter fluxes, ultimately triggering anoxic to euxinic conditions in the more restricted settings (Jenkyns, 2010).

According to these scenarios, changes in continental weathering likely played a central role in the genesis of anoxic conditions as well as in the subsequent drawdown of excess atmospheric  $\text{CO}_2$  (Cohen et al., 2004). The shift of strontium and osmium isotopes toward more radiogenic values at the top of the *tenuicostatum* Zone in Yorkshire has been taken as evidence for a dramatic increase of continental weathering rates at the onset of T-OAE (from 400 to 800% based on osmium-isotopes; Cohen et al., 2004). Nevertheless, it has been suggested that the strontium isotope shift could reflect decreased sedimentation rates in the studied localities (McArthur et al., 2000; Waltham and Gröcke, 2006; Hesselbo et al., 2007), whereas changes in osmium isotopes could reflect local basin restriction from the open-ocean (McArthur et al., 2008). In this context, the tempo and amount of changes in continental weathering during the early Toarcian remain highly debated, therefore limiting our understanding of the feedback mechanisms that operated after these pulses of massive carbon injection.

In this study, we present new  $\delta^{44/40}\text{Ca}$  measurements of well preserved brachiopods shells and bulk rock samples from the hemipelagic strata of Pliensbachian–Toarcian age of Peniche in Portugal. In order to reconstruct evolution of  $\delta^{44/40}\text{Ca}$  of seawater across early Toarcian interval, we constructed a one-box mass balance model to generate quantitative predictions for marine calcium isotopes associated with various scenarios proposed for the early Toarcian events.

## 2. Geological setting and stratigraphy

The analyzed samples have been collected from the Peniche section at Ponta do Trovão (GSSP candidate for Pliensbachian–Toarcian boundary) currently located on the Atlantic Portuguese coastline, in the Lusitanian Basin (Fig. 1). The Peniche section exposes a relatively continuous hemipelagic succession of early Pliensbachian to middle Toarcian age (Duarte et al., 2004; Elmi, 2006). The section benefits from high-resolution sedimentological, geochemical and ammonite biostratigraphic data (Elmi, 2006; Hesselbo et al., 2007; Suan et al., 2008a) that allow temporal correlation with other time-equivalent sections. The Peniche succession was deposited in a shallow epicontinental basin ( $\sim 200$  m; Bjerrum et al., 2001) near an emerged tilted block (Berlenga–Farilhães horst) (Duarte et al., 2004), which is relic of Lusitanian margin opening. During the early Toarcian, this area was connected to the Tethyan domain, the Boreal domain and to the proto-Atlantic corridor (central Atlantic opening) at tropical latitudes ( $20\text{--}30^\circ\text{N}$ ) (Fig. 1) (Huber et al., 2000).

The studied part of the Peniche succession comprises 48 m of marine strata from the top of *spinatum* zone (upper Pliensbachian) to the top of *levisoni* zone (early Toarcian) (Fig. 2). The argillaceous marls of the *levisoni* zone record a marked negative CIE characteristic of the T-OAE (Fig. 2), as well as high proportions of quartz, micas and feldspars (Suan et al., 2008a). The *levisoni* zone deposits are also characterized by occurrence of numerous silty to sandy turbidite levels (likely sourced from the Berlenga–Farilhães horst; Hesselbo et al., 2007). The total organic carbon contents are very low ( $\sim 0.5\%$ ; Hesselbo et al., 2007) for this section as compared to coeval, highly laminated and organic carbon-rich marine successions from other N–W European sections (Röhl et al., 2001; van Breugel et al., 2006; Jenkyns, 2010). However, the scarcity of bioturbation, benthic fauna and belemnites (‘belemnite gap’, Hesselbo et al., 2007) in the marls of the lower part of the *levisoni* zone suggests unfavorable conditions for animal life both at the seafloor and in the water column during the T-OAE (Hesselbo et al., 2007).

## 3. Materials and methods

### 3.1. Brachiopod preservation and sampling

The texturally well-preserved and non-luminescent parts of the shells studied by Suan et al. (2008a) were resampled for this study to obtain additional material for calcium isotope measurements. (See Table 1.) The shells were first washed with double deionized water, and the primary layer and the outer part of secondary layer, considered to be secreted out of isotopic equilibrium with oceanic water for carbon and oxygen (Auclair et al., 2003; Brand et al., 2003; Parkinson et al., 2005) but also calcium isotopes (Gussone et al., 2005; Von Allmen et al., 2010), were carefully removed with a dental scraper under binocular microscope. A few milligrams of unaltered fibrous calcite were extracted with an iron needle on parts of the shells without punctuations and specialized structures (posterior part of shell), which may also display values out of expected isotopic equilibrium (Carpenter and Lohmann, 1995; Auclair et al., 2003; Brand et al., 2003; Gussone et al., 2005). Due

**Table 1**

Isotope and elemental data measured in this study for samples collected in the Pliensbachian–Toarcian succession of Peniche.  $\delta^{44/40}\text{Ca}_{\text{SW}}$  correspond to the calcium isotope composition of seawater reconstructed using brachiopod data corrected for temperature and bulk carbonate corrected for variable contribution of dolomite assuming a difference between calcite and dolomite end-members of 2.2‰ (Rustad et al., 2010). See text for details about these corrections. Oxygen and carbon isotope data are from Suan et al. (2008a).

Samples	Height (m)	$\delta^{18}\text{O}$ PDB (‰)	$\delta^{13}\text{C}$ PDB (‰)	$\delta^{44/42}\text{Ca}$ raw (u.m.a. ‰)		Mean	2SD	$\delta^{44/40}\text{Ca}$ raw (‰)	2SD	$\delta^{44/42}\text{Ca}$ raw (‰)	$\delta^{44/42}\text{Ca}$ SRM915b (‰)	$\delta^{44/40}\text{Ca}$ SRM915b (‰)	$\delta^{44/40}\text{Ca}$ SRM915a (‰)	$\delta^{44/40}\text{Ca}$ SW SRM915b (‰)	$\delta^{44/40}\text{Ca}$ SW SRM915a (‰)	[Ca] (ppm)	[Mg] (ppm)	[Fe] (ppm)	
<i>Brachiopods</i>																			
BB11-1	4.47	-0.5	2.54	-0.07	-0.11			-0.09	0.04	-0.37	0.17	-0.19	0.03	0.07	0.79	0.95	1.64		
BB16	5.61	-0.89	2.18	-0.18	-0.16	-0.22	-0.21	-0.19	0.05	-0.77	0.19	-0.39	-0.17	-0.35	0.37	0.5	1.22		
BB13	6.09	-1.01	1.63	-0.31	-0.29			-0.3	0.02	-1.21	0.07	-0.61	-0.39	-0.81	-0.09	0.04	0.76		
BB43bis-1	8.63	-2.22	-0.11	-0.32	-0.25			-0.28	0.07	-1.13	0.27	-0.56	-0.34	-0.72	0.00	0.06	0.85		
Pen06 B1	8.63	-0.96	2.87	-0.11				-0.11		-0.45		-0.23	-0.01	0.71	0.84	1.56			
Pen06 B2	8.63	-1.49	2.02	-0.17	-0.18			-0.18	0.01	-0.71	0.04	-0.36	-0.14	-0.28	0.44	0.54	1.29		
Pen 05 BB45	9.2	-1.9	1.07	-0.15	-0.18	-0.18		-0.17	0.03	-0.66	0.11	-0.33	-0.11	-0.24	0.48	0.56	1.33		
Pen 05 B3bis	9.68	-1.67	2.99	-0.2	-0.23			-0.21	0.03	-0.85	0.12	-0.42	-0.2	-0.43	0.29	0.38	1.14		
BB46-2	10.35	-1.5	2.24	-0.21	-0.26			-0.24	0.05	-0.94	0.2	-0.47	-0.25	-0.53	0.19	0.29	1.04		
BB50-1	12.18	-1.3	3.51	-0.21				-0.21		-0.84		-0.42	-0.2	-0.42	0.3	0.41	1.15		
BB53	13.34	-1.36	3.82	-0.23	-0.25			-0.24	0.02	-0.94	0.08	-0.47	-0.25	-0.53	0.19	0.3	1.04		
B6-2	15.52	-1.69	3.72	-0.12				-0.12		-0.48		-0.24	-0.02	-0.04	0.68	0.77	1.53		
BB56	22.4	-2.53	0.53	-0.24	-0.25			-0.25	0.01	-0.99	0.06	-0.5	-0.28	-0.58	0.14	0.17	0.99		
BB29-2	30.37	-2.76	2.54	-0.08				-0.08		-0.34		-0.17	0.05	0.11	0.83	0.85	1.68		
BB32	31.16	-2.52	1.93	-0.13	-0.13			-0.13	0.00	-0.53	0.01	-0.26	-0.04	-0.09	0.63	0.66	1.48		
BB34	32.42	-2.36	3.13	-0.15				-0.15		-0.59		-0.29	-0.07	-0.15	0.57	0.61	1.42		
BB36-3	33.96	-2.09	3.51	-0.11				-0.11		-0.43		-0.21	0.01	0.01	0.73	0.79	1.58		
BB37	34.77	-2.19	4.05	-0.16	-0.16			-0.16	0.01	-0.64	0.03	-0.32	-0.1	-0.21	0.51	0.57	1.36		
BB20	38.62	-1.96	5.32	-0.07	-0.13			-0.1	0.06	-0.41	0.25	-0.2	0.02	0.03	0.75	0.83	1.61		
BB7-2	39.73	-2.23	5.54	-0.07	-0.14			-0.1	0.07	-0.41	0.27	-0.21	0.01	0.03	0.75	0.82	1.6		
BB25	45.62	-2.2	4.98	-0.17				-0.17		-0.69		-0.34	-0.12	-0.26	0.46	0.52	1.31		
<i>Bulk carbonate</i>																			
BB53	13.34			-0.26						-0.52		-0.3	-0.62	0.1	0.6	1.32	309 226	6432	5536
B6-2	15.52			-0.21						-0.42		-0.2	-0.43	0.29	0.79	1.51	403 861	6272	5440
476	18.058			-0.23						-0.47		-0.25	-0.52	0.2	0.7	1.42	308 195	6175	4502
159	20.664			-0.29						-0.59		-0.37	-0.77	-0.05	0.55	1.27	417 924	11968	10656
BB56	22.4			-0.48						-0.95		-0.74	-1.54	-0.82	-0.09	0.63	311 925	19777	10977
247	25.976			-0.36						-0.73		-0.51	-1.07	-0.35	0.19	0.91	285 851	8289	5665
524	28.864			-0.32						-0.64		-0.42	-0.87	-0.15	0.37	1.09	311 312	7850	4582
617	31.989			-0.21						-0.42		-0.43	0.29	0.89	1.61	431 471	11843	10819	
BB34	32.42			-0.26						-0.51		-0.29	-0.61	0.11	0.66	1.38	294 394	9318	6436
BB37	34.77			-0.25						-0.5		-0.28	-0.59	0.13	0.64	1.36	315 172	7104	7392

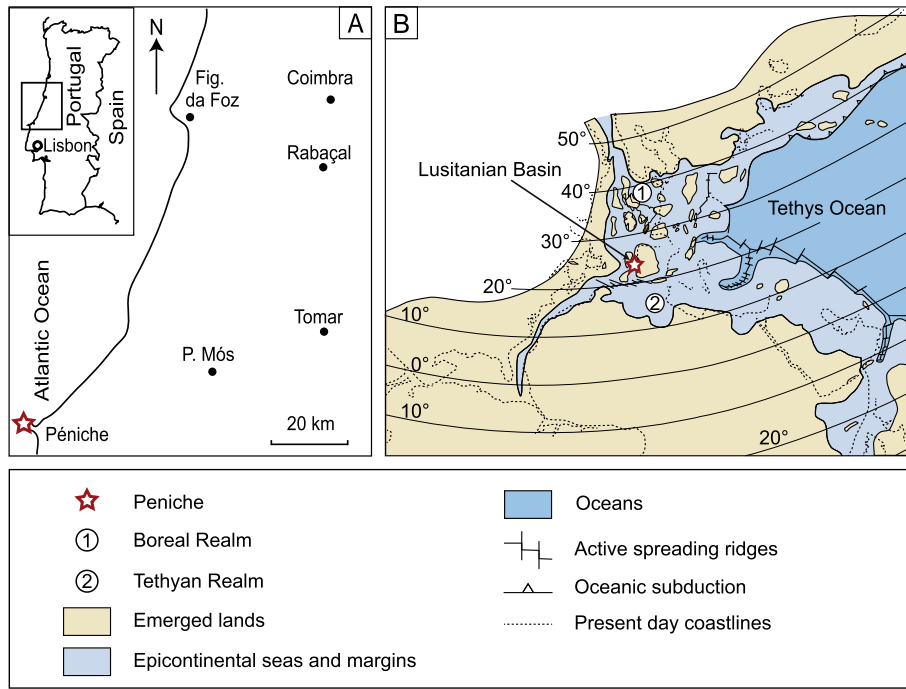


**Fig. 1.** Paleo- and geographical settings of studied section. (A) Location of the studied section; (B) Paleogeography of the western margin of the Tethys Ocean and location of the Lusitanian Basin (modified after Suan et al., 2008a, 2010).

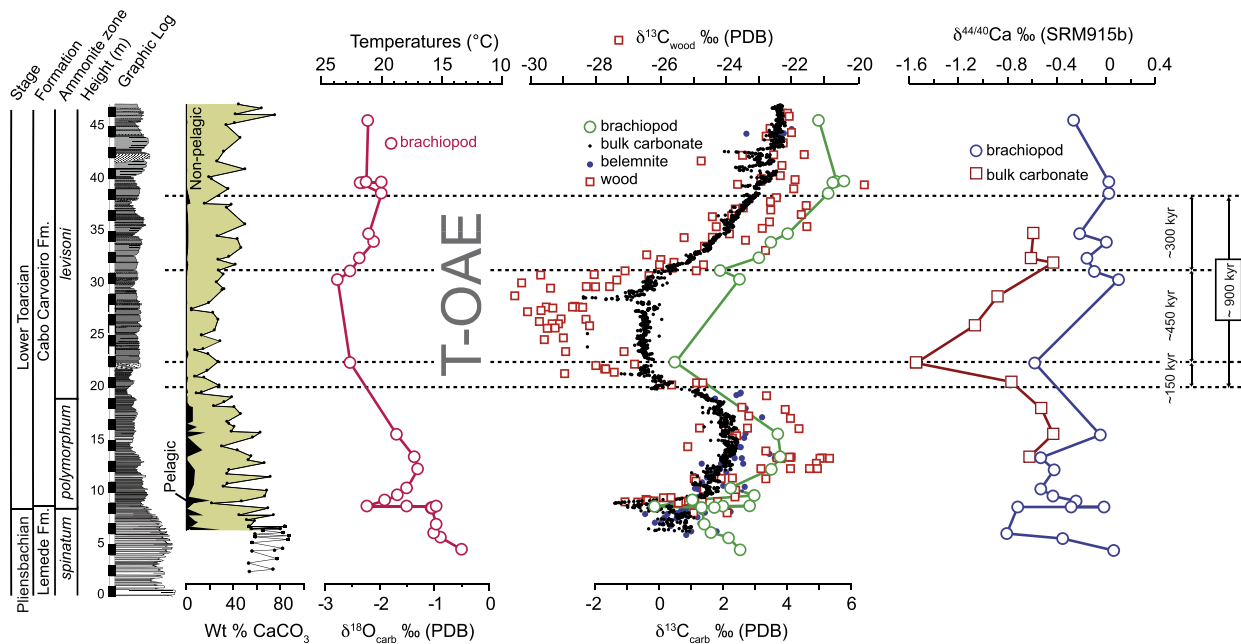


**Fig. 2.** Geochemical and micropaleontological data from the Pliensbachian–Toarcian age sediments of Peniche, Portugal. The  $\delta^{44/40}\text{Ca}$  (relative to SRM915b) ratio for bulk carbonates and brachiopod shells are from this study. Carbonate contents and quantification of pelagic nannofossils, brachiopod  $\delta^{18}\text{O}$  and  $\delta^{13}\text{C}$  ratios are from Suan et al. (2008a);  $\delta^{13}\text{C}$  of bulk carbonate, fossil wood and belemnites are from Hesselbo et al. (2007). Note the similarity between the  $\delta^{13}\text{C}$  and  $\delta^{44/40}\text{Ca}$  trends recorded by brachiopods shells and bulk carbonates.

to the thinness of the anterior part of their shell, the posterior part was also extracted in samples Pen 05 B3bis and BB50-1. The sampling quality was assessed by inspecting the polished shells with a Phenom™ G2 pure scanning electron in backscatter mode.

### 3.2. Bulk carbonate samples

Ten sediment samples were selected from the lower Toarcian interval in order to compare the calcium isotopic ratio of bra-

chiopod shell and bulk carbonates, the most commonly used substratum in previous calcium isotope studies of ancient events of environmental change (Payne et al., 2010; Blättler et al., 2011). Four of these bulk sediment samples come from the same horizons where brachiopods shells were collected (Table 2). Five more bulk carbonate samples were analyzed to fill the T-OAE interval, which has yielded only few brachiopod samples. Fragments of the micritic fraction without visible bioclasts and cements were powdered using an agate mortar and pestle. The  $\text{CaCO}_3$  content of these bulk

**Table 2**  
Possible  $\delta^{44/40}\text{Ca}$  values of dolomite and calcite end-members in bulk sediments at Peniche.

	$\delta^{44/40}\text{Ca}$ SRM915b (‰)
Case 1 <sup>a</sup>	
Calcite	−0.4914034
Dolomite	−7.9736034
Case 2 <sup>b</sup>	
Calcite	−0.4914034
Dolomite	−2.692

<sup>a</sup> Values calculated using the inverse relationship between  $\delta^{44/40}\text{Ca}$  ratios and dolomite contents shown in Fig. 4.

<sup>b</sup> Values obtained assuming the same  $\delta^{44/40}\text{Ca}$  ratios for calcite but a dolomite end member −2.2 ‰ lighter, as suggested by theoretical calculation of Rustad et al. (2010) for precipitation at 25 °C.

sediment samples was determined using a Dietrich–Frühling calimeter to facilitate calcium isotope measurements.

### 3.3. Analytical procedures

For each brachiopod sample, 0.2 mg of powder was directly dissolved in distilled 3.5N nitric acid ( $\text{HNO}_3$ ) in polypropylene microtubes. The bulk carbonate powders were dissolved in distilled 2N acetic acid at room temperature for 10 min and centrifuged at 4200 rpm during 15 minutes to remove clays and insoluble materials. The milliliter of supernatant of each sample was transferred into borosilicate glass tube and dried at 140 °C and dissolved again in distilled 3.5N  $\text{HNO}_3$ . All sample and standard (NIST SRM915b) solutions were loaded in ion-exchange chromatographic columns filled with Eichrom™ Sr-Spec resin to remove the strontium ions (Tacail et al., 2014). Indeed, strontium monatomic bivalent ions can create significant interferences with calcium ions signal due to their extremely close  $m/z$  ratio, and therefore compromise calcium isotope measurements for sample with Ca/Sr ratio lower than 10 000 (Morgan et al., 2011). After calcium elution with distilled 3.5N  $\text{HNO}_3$ , samples were collected into Teflon beakers and dried down at 70 °C for twelve hours. The calcium contents of two aliquots of 50  $\mu\text{l}$  taken before and after the chemical procedure of each sample were determined using a Thermo Electron iCAP 6000 series™ ICP-AES (Inductively coupled plasma atomic emission spectrometer) at the Laboratoire de Géologie de Lyon to ensure the complete recovery of the calcium ions. The purified bulk carbonate samples were distilled at 1.25 ppm in 0.5N  $\text{HNO}_3$  and their magnesium, iron and potassium contents were determined using the same spectrometer. The precision of the measurements, corrected for instrumental drift, was better than 98% based on the reproducibility of standard replicates. The Ca/metal of the solutions being >10 for all these elements, the one-step column chemistry described above was considered sufficient to avoid interference and matrix effects (Morgan et al., 2011) and allow reliable calcium isotope measurements.

The calcium isotope measurements were performed with a Thermoscientific Neptune Plus MC-ICP-MS (multi-collector inductively coupled plasma mass spectrometer) at the Laboratoire de Géologie de Lyon. Samples were prepared at 7 ppm Ca and introduced into an Aridus-II™ desolvator at a rate of 100  $\mu\text{L}/\text{min}$ , and the aerosol was carried into a hot plasma (RF power = 1200 W). The  $^{42}\text{Ca}$ ,  $^{43}\text{Ca}$  and  $^{44}\text{Ca}$  beam intensities were simultaneously measured and sample-standard bracketing was used with reference materials (NIST SRM915b) to derive  $\delta^{44}\text{Ca}$  ratios as

$$\delta^{44/42}\text{Ca} = \left( \frac{(^{44}\text{Ca}/^{42}\text{Ca})_{\text{sample}}}{(^{44}\text{Ca}/^{42}\text{Ca})_{\text{standard}}} - 1 \right) * 1000$$

Double charged strontium ions intensities were measured at mass 43.5 to correct direct interferences on the three other beams. Forty integrations of 4.2 s each were performed on every sample, followed by a washout phase of five minutes in 0.5N  $\text{HNO}_3$  and a five minutes conditioning in 0.05N  $\text{HNO}_3$ . Data quality was assessed by triple isotope  $\delta^{44/42}\text{Ca}$  versus  $\delta^{44/43}\text{Ca}$  plot following the procedure of Reynard et al. (2010). The average external reproducibility of  $\delta^{44/42}\text{Ca}$  measurements equaled internal reproducibility during the measurements session and was  $\pm 0.13\text{‰}$  (2SD) and  $\pm 0.10\text{‰}$  (2SE).

In this study, calcium isotopic ratios are expressed as  $\delta^{44/40}\text{Ca}$  relative to the NIST SRM915b reference materials. The  $\delta^{44/40}\text{Ca}$  values of SRM915b relative to SRM915a, the most commonly used reference material of previous calcium isotopes studies (Farkaš et al., 2007b; Payne et al., 2010; Blättler et al., 2011), is  $+0.72 \pm 0.04\text{‰}$  (Heuser and Eisenhauer, 2008). Values of  $\delta^{44/42}\text{Ca}$  can be converted to  $\delta^{44/40}\text{Ca}$  multiplying by mass fractionation ratio  $(1/m_{40} - 1/m_{44})/(1/m_{42} - 1/m_{44}) = 2.10$  (where  $m_x$  is the exact atomic mass of each calcium isotopes).

## 4. Results

### 4.1. $\delta^{44/40}\text{Ca}$ measurements

The measured  $\delta^{44/40}\text{Ca}$  ratios of brachiopod shells ( $\delta^{44/40}\text{Ca}_{\text{brachiopod}}$ ) show trends that are very similar to those recorded by their  $\delta^{13}\text{C}$  ratios (Suan et al., 2008a) throughout the studied stratigraphic interval (Fig. 2). The  $\delta^{44/40}\text{Ca}_{\text{brachiopod}}$  ratios decrease markedly from  $-0.02\text{‰}$  to  $-0.81\text{‰}$  across the PI–To boundary, broadly coincident with the shift towards lighter values in  $\delta^{13}\text{C}$  (2.87 to  $-0.11\text{‰}$ ) and  $\delta^{18}\text{O}$  ( $-0.96$  to  $-2.22\text{‰}$ ) recorded by the same brachiopods shells (Suan et al., 2008a). The  $\delta^{44/40}\text{Ca}_{\text{brachiopod}}$  ratios return to lighter values ( $-0.04\text{‰}$ ) in the middle of *polymorphum* zone, hence appearing as a broad 0.5–1‰ negative excursion. A second shift toward lighter  $\delta^{44/40}\text{Ca}_{\text{brachiopod}}$  values is recorded in the lowermost part of *levisoni* zone ( $-0.04$  to  $-0.58\text{‰}$ ) where a marked ( $\sim 3\text{‰}$ ) decrease of  $\delta^{13}\text{C}$  values is also recorded. The  $\delta^{44/40}\text{Ca}_{\text{brachiopod}}$  ratios increase again in the second half of the *levisoni* zone and reach their maximum values ( $0.17\text{‰}$ ) in the uppermost part of *levisoni* zone, where maximum  $\delta^{13}\text{C}$  values are also recorded.

The stratigraphic trends of bulk carbonate  $\delta^{44/40}\text{Ca}$  values ( $\delta^{44/40}\text{Ca}_{\text{bulk}}$ ) are very similar to that recorded by brachiopods. The  $\delta^{44/40}\text{Ca}_{\text{bulk}}$  values are systematically lighter than  $\delta^{44/40}\text{Ca}_{\text{brachiopod}}$  values, even if the difference is not constant through the studied interval (Fig. 2). The two stratigraphically lowest samples record a shift toward heavier  $\delta^{44/40}\text{Ca}$  values ( $-0.62\text{‰}$  to  $-0.43\text{‰}$ ) at the top of the *polymorphum* zone similar to that recorded by the brachiopods from the same horizons. The  $\delta^{44/40}\text{Ca}_{\text{bulk}}$  ratios decrease markedly and gradually across the *polymorphum*–*levisoni* transition, reaching their minimum values ( $-1.54\text{‰}$ ) in the basal *levisoni* zone and return to pre-excursion values in the middle of the *levisoni* zone (Fig. 3). The amplitude of the  $\delta^{44/40}\text{Ca}_{\text{bulk}}$  negative excursion ( $-1.11\text{‰}$ ) is twice as large as that recorded by brachiopods ( $-0.54\text{‰}$ ) through the T–OAE interval.

### 4.2. Magnesium and iron contents in bulk carbonate

The Mg and Fe contents show trends similar to those reported by Hermoso et al. (2009), albeit showing somewhat lower values in the basal *levisoni* Zone (Fig. 3). The Fe and Mg contents, expressed as a proportion of the carbonate, show minimum values in samples from the *polymorphum* Zone (4502 ppm for Fe and 6175 ppm for Mg) and increase markedly across the *polymorphum*–*levisoni* transition. The Fe and Mg contents reach maximum

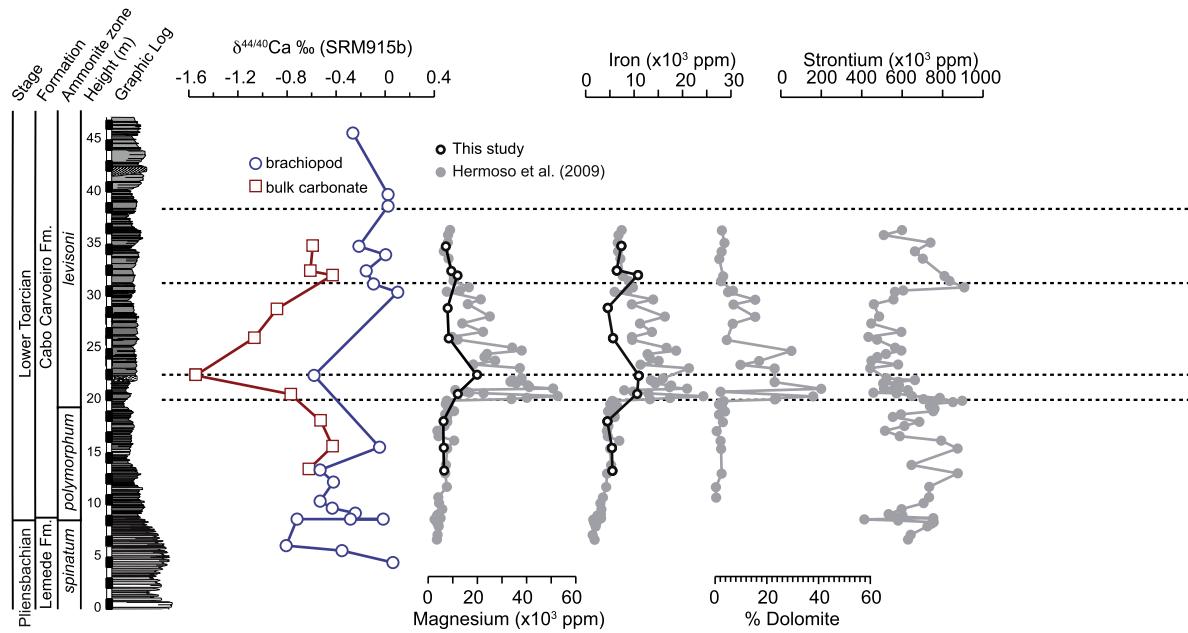


**Fig. 3.**  $\delta^{44/40}\text{Ca}$  (relative to SRM915b) ratio for bulk carbonates and brachiopod shells compared to Mg, Fe, dolomite and Sr contents of the bulk carbonate phase from the same Pliensbachian–Toarcian succession at Peniche. The lowest  $\delta^{44/40}\text{Ca}$  values for bulk carbonates correspond to highest Mg and dolomite contents indicate that higher dolomite content may partly explain the recorded trends. The low Sr contents at the Pl–To and T–OAE intervals suggest that the aragonite contribution to the bulk carbonate was minimum at the corresponding time intervals.

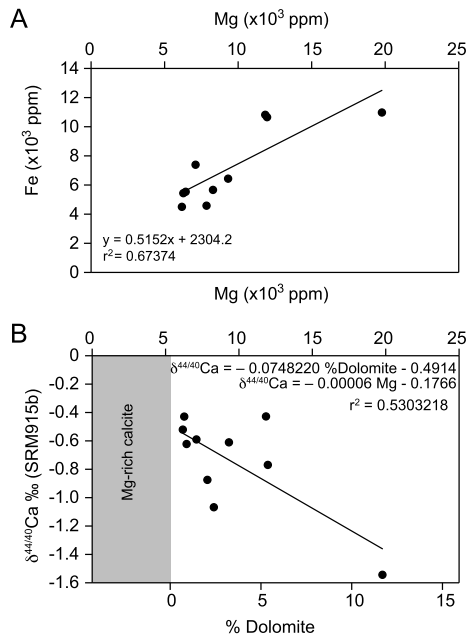


**Fig. 4.** (A) Cross-plots of Mg vs. Fe contents (B)  $\delta^{44/40}\text{Ca}_{\text{bulk}}$  vs. Mg contents and dolomite contents. Dolomite contents were derived from Mg contents of this study using the relationship  $\text{wt.\% Dolomite} = 0.0008 * \text{Mg} - 4.2073$  ( $r^2 = 0.97$ ) reported by Hermoso et al. (2009) for the same section.

values (10976 ppm for Fe and 19777 ppm for Mg) in the basal *levisoni* zone, decrease in the middle of *levisoni* zone and record a second peak in the second half part of the *levisoni* zone (4581 to 10818 ppm for Fe and 7850 to 11843 ppm for Mg). As shown for the same succession by Hermoso et al. (2009), Mg content correlates positively with Fe content (Fig. 4); Mg content also shows a moderately good inverse linear correlation with the  $\delta^{44/40}\text{Ca}_{\text{bulk}}$  ratios (Fig. 4).

## 5. Discussion

### 5.1. Diagenesis and calcium carbonate origin

Several studies have suggested that  $\delta^{44/40}\text{Ca}$  of biogenic calcite reflects the isotopic composition of seawater where it was formed (De LaRocha and DePaolo, 2000; Schmitt et al., 2003), and more particularly in the case of calcite coming from secondary layer of the brachiopods shell. No structural evidence for diagenetic phenomena have been observed during the inspection of brachiopod specimens under SEM and cathodoluminescence analyses (Suan et al., 2008a), pointing to an unaltered primary isotopic signal.

Modern articulated brachiopods precipitate their shell close to calcium isotope equilibrium with surrounding seawater (Von Allmen et al., 2010), which has spatially uniform  $\delta^{44/40}\text{Ca}$  composition throughout modern oceans (Hippler et al., 2003). Assuming that Early Jurassic brachiopods also precipitated their shell in isotopic equilibrium, our record would hence reflect global changes in  $\delta^{44/40}\text{Ca}_{\text{seawater}}$  through the studied interval. Nevertheless, transient isolation of the Lusitanian Basin from the open sea may have deviated the seawater  $\delta^{44/40}\text{Ca}$ , as suggested for Ordovician epeiric settings (Holmden, 2009). Temporary isolation would, however, have also impacted other isotopic systems (Holmden, 2009; Payne et al., 2010) and is not supported by available data. For instance, transient increases in freshwater contribution, which might have locally lowered the seawater  $\delta^{44/40}\text{Ca}$ , would have also increased seawater  $^{87}\text{Sr}/^{86}\text{Sr}$  ratios; this scenario is at odds with the belemnite  $^{87}\text{Sr}/^{86}\text{Sr}$  record of Peniche (Hesselbo et al., 2007), which is indistinguishable from that of UK (McArthur et al., 2000) and Canada (Caruthers et al., 2011). In addition, local restriction would have impacted more severely the isotope composition of elements with shorter residence times, such as carbon and oxygen (Holmden, 2009); nevertheless, the similarity between the  $\delta^{18}\text{O}$  and  $\delta^{13}\text{C}$  values recorded by the brachiopod shells at Peniche and that recorded by belemnites and bulk carbonate from several coeval sites (McArthur et al., 2000; Bailey et al., 2003; van de Schootbrugge et al., 2005; Sabatino et al., 2009; Harazim et al., 2013) suggest good connection with adjacent basins and

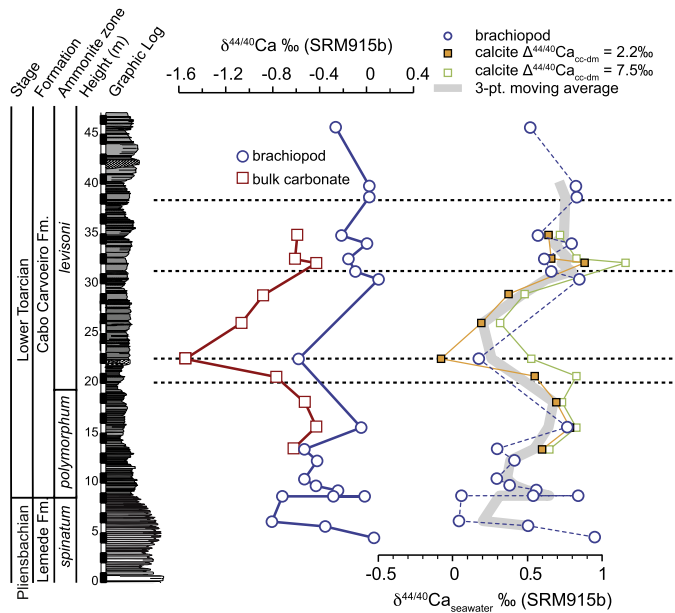


**Fig. 5.**  $\delta^{44/40}\text{Ca}$  of bulk carbonate and brachiopod shells through the Pliensbachian–Toarcian succession at Peniche and reconstruction of the  $\delta^{44/40}\text{Ca}_{\text{seawater}}$ . Reconstructed  $\delta^{44/40}\text{Ca}_{\text{seawater}}$  values are based on bulk carbonate values corrected for dolomite contribution using the different  $\delta^{44/40}\text{Ca}$ -dolomite end-members listed in Table 2 and brachiopods shell values corrected from temperature effect. The grey line represents a 3-point moving average of brachiopod-derived  $\delta^{44/40}\text{Ca}_{\text{seawater}}$  values and bulk carbonate-derived values using a dolomite end-member 2.2‰ lighter than calcite.

also invalidates this hypothesis. Since our record corresponds to one of the deepest parts of the basin, it therefore appears that the variations of the  $\delta^{44/40}\text{Ca}$  values recorded by the brachiopod shells from Peniche captures regional, if not global, changes in seawater  $\delta^{44/40}\text{Ca}$  rather than local effects affecting only the Lusitanian Basin.

The bulk carbonate phase represents a complex admixture of several sources and is thus more likely to reflect compositional biases. At Peniche, bulk carbonate is dominated by a non-pelagic micritic fraction (Fig. 2; Suan et al., 2008a) but also contains fine-grained ferroan dolomite that may exceed 40% of the bulk carbonate in the *levisoni* Zone (Fig. 3; Hermoso et al., 2009). This dolomite fraction likely precipitated in pore fluids under oxygen- and sulfate-depleted conditions during early diagenesis (Hermoso et al., 2009) and shows a strong positive correlation ( $r^2 = 0.96$ ) with the Mg contents (Hermoso et al., 2009). The moderately good, inverse relationship recorded between  $\delta^{44/40}\text{Ca}_{\text{bulk}}$  and Mg contents at Peniche (Figs. 3 and 4) therefore suggests that changes in dolomite contribution may represent a major source of  $\delta^{44/40}\text{Ca}_{\text{bulk}}$  variability.

In order to assess the potential influence of these changes in dolomite contribution to the  $\delta^{44/40}\text{Ca}_{\text{bulk}}$  signal, we have calculated the  $\delta^{44/40}\text{Ca}$  values of the dolomite and calcium end-members (Table 2; Fig. 5) using the dolomite– $\delta^{44/40}\text{Ca}_{\text{bulk}}$  relationship (Fig. 4). Although the direction of  $\delta^{44/40}\text{Ca}$  changes between dolomite and calcite is in line with that suggested by Holmden (2009) for Ordovician dolostones (but see Blättler et al., 2011 and Fantle and Higgins, 2014), the obtained difference of  $\sim 7.5\text{‰}$  between dolomite and calcite ( $\Delta^{44/40}\text{Ca}_{\text{cc-dm}}$ ) is considerably larger than that suggested by previous studies (0.6‰ in Holmden, 2009; 2.2‰ in Rustad et al., 2010). We note that the ferroan dolomite at Peniche, in contrast to the late-stage dolomite studied by most previous authors (Holmden, 2009; Blättler et al., 2011), likely formed early during diagenesis, while the effect of dolomite precipitation on  $\delta^{44/40}\text{Ca}$  values remains a complex and poorly understood issue (Fantle and Higgins, 2014). Given the limited number of

Mg– $\delta^{44/40}\text{Ca}$  pairs in our dataset it is yet premature to speculate about the reasons behind this very large  $\Delta^{44/40}\text{Ca}_{\text{cc-dm}}$  value. Indeed, the  $\delta^{44/40}\text{Ca}$  dolomite end-member ( $-7.9\text{‰}$ ) implied by the Mg– $\delta^{44/40}\text{Ca}$  relationship is considerably lower than any natural carbonate  $\delta^{44/40}\text{Ca}$  value measured so far (Coplen et al., 2002), and thus appears rather unrealistic. The Mg– $\delta^{44/40}\text{Ca}$  relationship may, however, still be justified with a non-pure dolomite end-member or considering smaller  $\Delta^{44/40}\text{Ca}_{\text{cc-dm}}$  values. Assuming a range of various  $\Delta^{44/40}\text{Ca}_{\text{cc-dm}}$  values (Table 2), we have calculated changes in  $\delta^{44/40}\text{Ca}$  that are not explained by dolomite contribution (Fig. 4). The obtained values still depict a marked negative  $\delta^{44/40}\text{Ca}$  excursion, but this latter is smaller in amplitude ( $\sim 0.7$  to  $0.5\text{‰}$ ) compared to that (1.2‰) evident from the untreated  $\delta^{44/40}\text{Ca}$  values and more similar to that recorded by brachiopods (Fig. 4).

Apart from dolomite contribution, changes in the relative proportions of aragonite and calcite within the micritic fraction are also able to produce large changes in the  $\delta^{44/40}\text{Ca}$  values of bulk carbonate (Blättler et al., 2011). It has been proposed that a change from an aragonite to a calcite sea took place near the Early–Middle Jurassic transition (Sandberg, 1983; Stanley and Hardie, 1998), although this transition is poorly constrained and may have taken place before the Sinemurian (Dickson, 2004). In any case, such a shift in mineralogy would have increased the proportion of calcite relative to aragonite in oozes precipitated in carbonate platforms (Schlager and James, 1978) and exported to the Lusitanian Basin. Because aragonite is  $\sim 0.6\text{‰}$  isotopically lighter than calcite (Gussone et al., 2005), one would expect that the calcite-dominated bulk samples would have higher  $\delta^{44/40}\text{Ca}_{\text{bulk}}$  values during this transition, at odds with the decrease in  $\delta^{44/40}\text{Ca}_{\text{bulk}}$  values recorded in the basal *levisoni* Zone (Fig. 2). Conversely, we rule out the transient dominance of  $^{40}\text{Ca}$ -enriched aragonite mud production in platforms surrounding the Lusitanian Basin as the main cause of the T–OAE  $\delta^{44/40}\text{Ca}_{\text{bulk}}$  excursion, since the proportion of strontium relative to carbonate, which is expected to be higher in originally aragonite-rich sediments, shows its lowest values in T–OAE interval (Fig. 4; Hermoso et al., 2009).

## 5.2. Reconstruction of the $\delta^{44/40}\text{Ca}_{\text{seawater}}$ variations

In order to reconstruct the  $\delta^{44/40}\text{Ca}_{\text{seawater}}$  variations from the  $\delta^{44/40}\text{Ca}$  values of the brachiopod shells, it is essential to take into account the fractionation factor  $\alpha_{\text{cc/sw}}$  between calcite and seawater, which is expressed by the relation:

$$\alpha_{\text{cc/sw}} = (\delta^{44/40}\text{Ca}_{\text{calcite}} + 1000) / (\delta^{44/40}\text{Ca}_{\text{seawater}} + 1000)$$

where  $\delta^{44/40}\text{Ca}_{\text{calcite}}$  and  $\delta^{44/40}\text{Ca}_{\text{seawater}}$  represent the isotopic compositions of the brachiopod shells and seawater respectively (Heuser et al., 2005).

This fractionation factor was determined as  $\sim 0.99915$  for modern specimens of the brachiopod *Terebratalia* (Gussone et al., 2005) and it was retained for all brachiopods in this study. Besides, the calcium isotopic composition of modern brachiopod shells also shows a slight temperature dependency of  $\sim 0.016\text{‰}/^\circ\text{C}$  (Farkaš et al., 2007a). Consequently, the  $\delta^{44/40}\text{Ca}_{\text{seawater}}$  curves (Fig. 4) have been corrected using bottom-seawater temperatures reconstructed from the  $\delta^{18}\text{O}$  values of the measured brachiopod shells, which suggest an increase of  $\sim 5^\circ\text{C}$  at the PI–To and of  $\sim 7^\circ\text{C}$  during the T–OAE (Suan et al., 2008a). Because the sensitivity of the  $\delta^{44/40}\text{Ca}$  of brachiopods to temperature is weak and points to heavier values when temperature increases, the corrected profile shows slightly higher amplitudes for the PI–To (from 0.78 to 0.80‰) and the T–OAE (from 0.54 to 0.6‰) negative excursions than reflected in the raw data. However, the reconstructed  $\delta^{44/40}\text{Ca}_{\text{seawater}}$  profile shows similar trends to the brachiopods and indicates that the negative isotopic excursions cannot be explained by fractionation

changes between seawater and calcite due to globally warmer conditions.

The isotopic composition of the seawater has also been reconstructed using  $\delta^{44/40}\text{Ca}_{\text{bulk}}$  values corrected for dolomite contribution (Fig. 4) and a  $\Delta_{\text{carb}}$  of  $-1.2\text{‰}$  (assuming a proportion of 50% calcite and 50% aragonite crystallization on the platform; Blättler et al., 2012), representing the difference due to fractionation between calcium removal from the ocean and seawater. The reconstructed  $\delta^{44/40}\text{Ca}_{\text{seawater}}$  values for the T-OAE interval are based on both brachiopod and bulk carbonate data and are therefore relatively well constrained (Fig. 5). On the contrary, the reconstructed  $\delta^{44/40}\text{Ca}_{\text{seawater}}$  ratios near the Pl-To transition are supported only by brachiopod data and lack longer-term pre-excursion values. Further investigations are thus needed to produce more reliable  $\delta^{44/40}\text{Ca}_{\text{seawater}}$  reconstructions for this interval. However, given the number of geochemical similarities shared by the T-OAE and Pl-To intervals (Hesselbo et al., 2007; Suan et al., 2008a), the two calcium isotope excursions have been considered of equivalent magnitude in the following sections as a working hypothesis.

### 5.3. Potential causes of variations in the $\delta^{44/40}\text{Ca}_{\text{seawater}}$ record

According to previous models (Payne et al., 2010; Blättler et al., 2011) four different patterns of global environmental change could lead to a negative anomaly of the  $\delta^{44/40}\text{Ca}_{\text{seawater}}$  in response to geologically short events. The first of these is a shift from aragonite- to calcite-dominated carbonate deposition. Indeed, the calcite is isotopically heavier than aragonite in a range of  $0.6\text{‰}$  showing average  $\delta^{44/40}\text{Ca}$  values of  $-1\text{‰}$  (versus  $-1.7\text{‰}$  for aragonite) on modern carbonate (Blättler et al., 2012). Thus a change to globally significant calcite-dominated carbonate deposition could leave the seawater enriched in lighter isotope and generate a shift toward lower  $\delta^{44/40}\text{Ca}_{\text{seawater}}$  values. This hypothesis is however inconsistent with published Mg/Ca ratios of Mesozoic echinoderms, which suggest that the transition to a calcite-dominated sea probably took place before the Sinemurian, i.e., millions of years before the considered interval (Dickson, 2004). Furthermore, such a change in calcium isotope fractionation between seawater and carbonate should create a long-term (several Myr) shift of  $\delta^{44/40}\text{Ca}_{\text{seawater}}$  values (Hinojosa et al., 2012) and is thus at odds with the rapid ( $<1$  Myr) return to pre-excursion values few hundred thousand years after the Pl-To and T-OAE intervals at Peniche.

The second scenario is a global change in the isotope compositions of river ( $\delta^{44/40}\text{Ca}_{\text{river}}$ ) associated with no changes in their flux. However, it has been shown that the decrease of the  $\delta^{44/40}\text{Ca}_{\text{river}}$  necessary to explain a  $0.3\text{‰}$  negative excursion of  $\delta^{44/40}\text{Ca}_{\text{seawater}}$  occurring in less than 500 kyr would be out of the documented range of the  $\delta^{44/40}\text{Ca}$  for both weathered sedimentary or endogenous rock (Payne et al., 2010). Besides, this scenario would be inconsistent with the hypothesis that rivers should have relatively constant  $\delta^{44/40}\text{Ca}$  compositions over  $\sim 1$  Myr timescales (Schmitt et al., 2003).

The third possible scenario is a global decrease in carbonate deposition (ocean acidification) resulting from a massive input of carbon from crustal reservoirs (volcanism, methane hydrates), which would leave the ocean enriched in the lighter isotopes (Payne et al., 2010). This explanation is consistent with growing paleontological and sedimentological evidence showing a major biological crisis of highly calcified organisms, decrease in carbonate accumulation in the sedimentary basins and a drastic size reduction of pelagic producers at the onset of the T-OAE (Cohen et al., 2007; Suan et al., 2008a; Mattioli et al., 2009; Jenkyns, 2010; Treccalli et al., 2012). Nonetheless, the box modeling results of Blättler et al. (2011) indicate that a 90% reduction in the carbonate sink flux produces only a weak  $0.08\text{‰}$  negative  $\delta^{44/40}\text{Ca}_{\text{seawater}}$  excursion,

suggesting that this mechanism alone cannot explain the  $\delta^{44/40}\text{Ca}_{\text{seawater}}$  excursions reconstructed from our data.

The last conceivable scenario is a substantial increase in global continental weathering rates and hence in riverine flux bringing dissolved  $^{40}\text{Ca}$ -enriched calcium to the oceans. Previous models have shown that a 300% increase in riverine flux within 0.5 to 1 Myr is able to produce a  $0.2$  to  $0.4\text{‰}$  negative  $\delta^{44/40}\text{Ca}_{\text{seawater}}$  excursion (Blättler et al., 2011). This mechanism along with 'ocean acidification', would be the logical consequence of the massive input of carbon to the superficial reservoirs (e.g. Payne et al., 2010). In this regard, these two latter scenarios are advantageous in that they both account for the available geological evidence and the parallelism recorded between the carbon and calcium isotopes curves (Fig. 2).

### 5.4. Modeling the seawater calcium isotope negative excursions and implications for the causes and consequences of the T-OAE

In order to explore quantitatively the variation of seawater calcium isotopes throughout studied time interval, the Early Jurassic Ocean has been treated as a single box (Supplementary Material) with the main inputs of calcium to the ocean being riverine flux and hydrothermal alteration and the main sink being the seafloor carbonate deposition (DePaolo, 2004; Fantle and DePaolo, 2005). The modeled scenarios that best fit the  $\delta^{44/40}\text{Ca}_{\text{seawater}}$  curves reconstructed from Peniche are those involving large increases in continental weathering (500% and 1000%; Fig. 6). Given the ample sedimentological and paleontological evidence for decreased carbonate production and accumulation during both events (see Section 5.3), we favor a major decrease in carbonate burial ('ocean acidification') followed by the more conservative 500% increase in continental weathering as the most likely scenario explaining our  $\delta^{44/40}\text{Ca}$  data (Fig. 6).

The substantial increases in continental weathering suggested by our favored scenario for the Pl-To and T-OAE events are consistent with multiple lines of evidence. The here proposed 500% increase in continental weathering is indeed comparable to the 400 to 800% rise suggested by Cohen et al. (2004) on the basis of osmium isotope measurements from the Yorkshire coast ( $^{187}\text{Os}/^{188}\text{Os}$ ). Although supported by only one  $^{187}\text{Os}/^{188}\text{Os}$  measurement, these data also point to a shift toward radiogenic values in the lowermost part of the *tenuicostatum* Zone (Cohen et al., 2004) and are thus consistent with the large increase in weathering suggested by our  $\delta^{44/40}\text{Ca}$  data across the Pl-To interval. The large shift toward more radiogenic values recorded by strontium isotope data across the *exaratum* Subzone in Yorkshire has been also proposed to reflect a substantial increase in continental weathering at the onset of the T-OAE (Cohen et al., 2004). Nevertheless, the interpretation of these data is complicated by the likelihood that the Sr cycle was in a non-steady state during the Early-Middle Jurassic (Waltham and Gröcke, 2006); as such controversies about the duration of the involved segments of the curve (Suan et al., 2008a; Kemp et al., 2011; Huang and Hesselbo, 2013; Bouilila et al., 2014) compromise any quantitative interpretation of the Sr isotope data. Regardless of this debate, the large increase in kaolinite contents recorded at the base of the *serpentinum* Zone in NW Europe also corroborates a substantial acceleration of the riverine flux during the T-OAE (Dera et al., 2009).

The large increase in the riverine water input proposed for both events implies substantial increases in nutrient discharge to oceanic and coastal areas. Higher nutrient supply is in line with most proposed models for the T-OAE, and supported by the widespread occurrence of organic-rich sediments at the base of the *levisoni* Zone or its time-equivalent zones in many epicontinental areas worldwide (Jenkyns, 1988; Al-Suwaidi et al., 2010; Suan et al., 2011). Nevertheless, evidence for relatively well-oxygenated

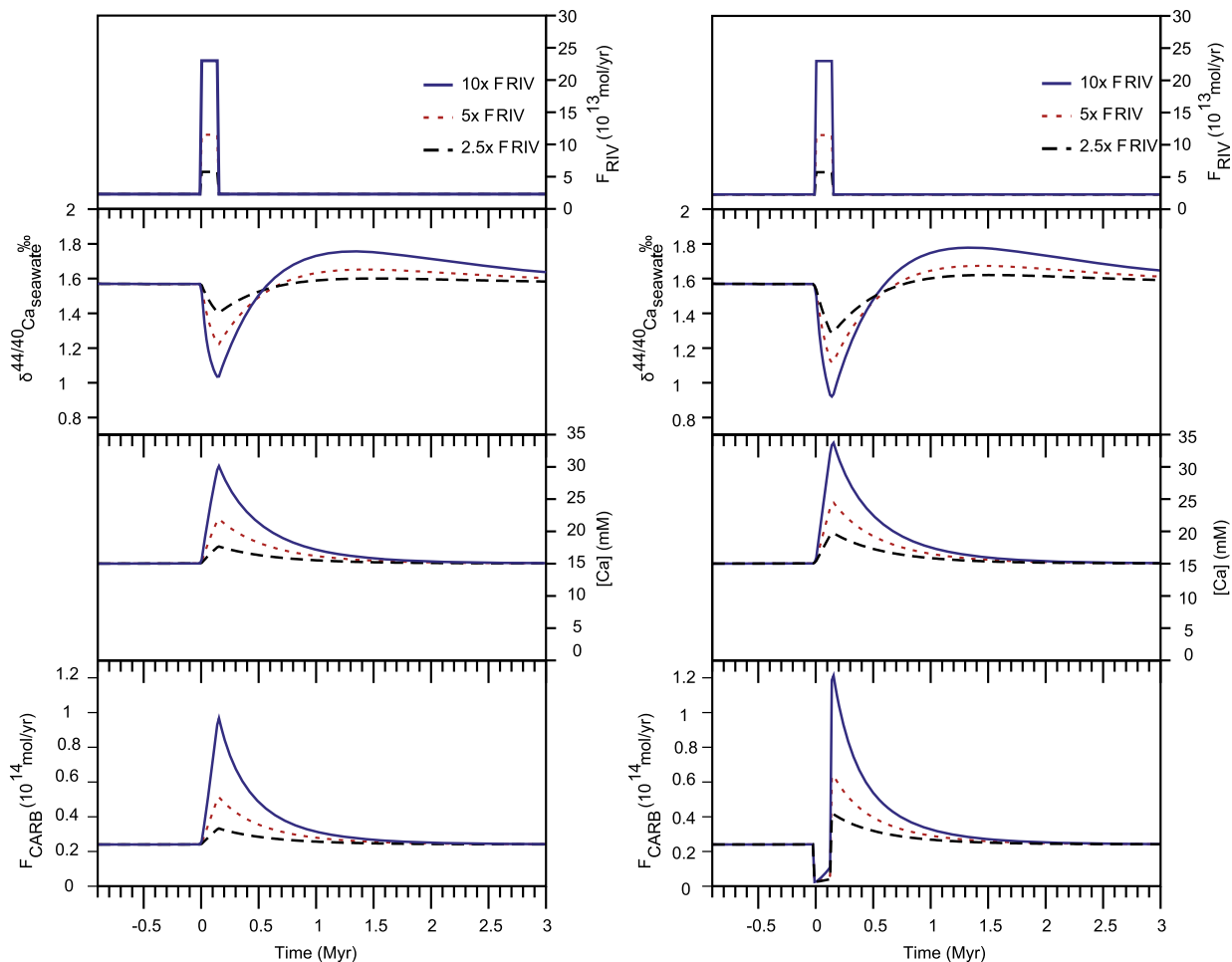


**Fig. 6.** Models results for two hypothetical forcing arrangements describe in the main text as ‘continental weathering’ and ‘ocean acidification + continental weathering’ scenarios. The time axis marks millions of years from the onset of the perturbation.  $F_{RIV}$  and  $F_{CARB}$  are riverine and carbonate fluxes and [Ca] is the calcium content of seawater. The baseline seawater value of 1.55‰ (NIST SRM915a) used in the model is based on the calcium isotope reconstruction of seawater presented in Fig. 5. The left panels (‘continental weathering’) show the behavior of the calcium isotope ratio, the calcium concentration in seawater and  $F_{CARB}$  when the  $F_{RIV}$  is increased by 2.5, 5 and 10 times at  $t = 0$  remaining elevated during 150 kyr. The right panels (‘ocean acidification + continental weathering’) show higher amplitude of calcium isotope excursions, calcium concentration in seawater and carbonate deposition ( $F_{CARB}$ ) when  $F_{CARB}$  is decreased by 90% at  $t = 0$  during 20 kyr before a 2.5, 5 and 10 times increase of  $F_{RIV}$  remaining elevated during 150 kyr. All the isotopic ratios used in the model are expressed as  $\delta^{44/40}\text{Ca}$  relative to the NIST SRM915a (see Section 3.3) to facilitate comparisons with previous calcium box-modeling studies.

conditions in several marine records of the T-OAE (including Peniche) indicates that the development of anoxia as a response to increased riverine input was strongly modulated by local conditions such as the depth, geometry or hydrology of the considered basins (Jenkyns, 2010; Gómez and Goy, 2011). Similar processes may be invoked to explain why organic-rich sediments dating from the earliest Toarcian (i.e., *polymorphum* Zone) have been reported from only a couple of localities in NW Europe (Röhl et al., 2001; Littler et al., 2010). Alternatively, the corresponding strata may have been winnowed or eroded by sea-level changes, as suggested by the frequent presence of hiatuses in strata recording the PI–To transition in NW European strata (Howard, 1985; Wignall, 1991; Morard et al., 2003; Pittet et al., 2014).

It is commonly admitted that chemical erosion is linearly correlated to physical erosion (Gaillardet et al., 1999). Accordingly, our conservative estimate of a 500% increase in continental weathering during the PI–To and T-OAE intervals implies a massive discharge of terrigenous sediments to the oceanic reservoir during both the PI–To and T-OAE intervals. At Peniche, an increase in sediment supply at the onset of the T-OAE is supported by the appearance of turbidites at the base of the *levisoni* Zone, which coincide with the fall of both  $\delta^{44/40}\text{Ca}_{\text{seawater}}$  and  $\delta^{13}\text{C}$  values (Hesselbo et al., 2007). Although turbiditic levels do not occur across the PI–To

transition at Peniche, a drastic increase in terrigenous supply during the equivalent time interval is recorded in the Dades–Thodra valley in Morocco where the *polymorphum* Zone is extremely expanded (>100 m) and exposes numerous siliciclastic turbiditic levels (Krencker et al., 2013).

In most earth system models, the continental weathering and carbonate deposition are linked at first order by a positive feedback involving the massive input of  $\text{Ca}^{2+}$  and  $\text{CO}_3^{2-}$  ions by river that increases oceanic alkalinity and thus saturation with respect to  $\text{CaCO}_3$  (Kump et al., 2009; Hönisch et al., 2012). In our models, this increasing burial of  $^{40}\text{Ca}$ -enriched sediments causes the return of  $\delta^{44/40}\text{Ca}_{\text{seawater}}$  values to pre-excursion values a few hundred thousand years after the onset of the perturbation (Fig. 6). This modeled increase in carbonate burial after the PI–To event is broadly consistent with the increase in  $\text{CaCO}_3$  contents and nannofossil fluxes at Peniche, which occur a few meters above the PI–To boundary (Fig. 2; Mattioli et al., 2008, 2009; Suan et al., 2010). Calcium carbonate contents and nannofossil fluxes also increase above the T-OAE interval at Peniche (Fig. 2) and in many other European basins, generally reaching their maximum values near or above the peak of the positive excursion following the T-OAE (Mattioli et al., 2004, 2008, 2009). According to all cyclostratigraphic estimates (Suan et al., 2008b; Kemp et al., 2011; Huang and Hesselbo, 2013;

**Table 3**

Instantaneous carbon mass-balance calculation using different reservoir sizes and isotopic compositions. Isotopic composition of the DIC (a) come from [Dickens et al. \(1995\)](#) and has been tested with a potential error of  $\pm 2\%$ . This calculation necessitates also an estimation of the early Pliensbachian DIC reservoir size, which has been modeled to be in the order of 84600 to 101 520 Gt (where 1 Gt =  $10^{15}$  g) ([Ridgwell, 2005](#)).

		Parameter		Value	
		$M_p$ PI-To and T-OAE (Gt)		40000	
		$\Delta\delta^{13}\text{C}$ T-OAE (‰ PDB)		3.287	
		$\Delta\delta^{13}\text{C}$ PI-To (‰ PDB)		2.65	
$M_i$ (Gt)	$\delta^{13}\text{C}_i$ (‰ PDB)	$\delta^{13}\text{C}_f$ PI-To (‰ PDB)	$\delta^{13}\text{C}_f$ TOAE (‰ PDB)	$\delta^{13}\text{C}_p$ PI-To (‰ PDB)	$\delta^{13}\text{C}_p$ T-OAE (‰ PDB)
84600	-2	-4.65	-5.287	-10.3	-12.2
84600	0 <sup>a</sup>	-2.65	-3.287	-8.3	-10.2
84600	2	-0.65	-1.287	-6.3	-8.2
101 520	-2	-4.65	-5.287	-11.4	-13.6
101 520	0 <sup>a</sup>	-2.65	-3.287	-9.4	-11.6
101 520	2	-0.65	-1.287	-7.4	-9.6

[Boullila et al., 2014](#)), this recovery in carbonate accumulation took place at least several hundred kyrs after the onset of the T-OAE, and is thus at odds with the peak in carbonate accumulation simulated by our models a few kyrs after the perturbation. This mismatch cannot be attributed to an overestimation of the T-OAE duration, since a  $\delta^{44/40}\text{Ca}$  excursion with a shorter duration (e.g., [Boullila et al., 2014](#)) would necessarily require briefer pulses of Ca input, and hence a peak in alkalinity occurring even sooner after the onset of the perturbation. In other words, any simulation of carbonate accumulation during these events requires the near coincidence of maximum rates of carbonate accumulation and minimum  $\delta^{44/40}\text{Ca}$  ratios to account for the rapid return to pre-excursion  $\delta^{44/40}\text{Ca}$  excursions values recorded at Peniche.

This long recovery time could be attributed to the epicontinental setting of most T-OAE sites studied so far, where elevated nutrient load may have delayed the recovery of calcification in both neritic and pelagic settings. Carbonate accumulation may then have taken place mostly as in remote carbonate platforms during the T-OAE, as suggested by the chemostratigraphic study of massive carbonate platform oolitic limestone beds in Italy ([Trecalli et al., 2012](#)). Alternatively, high alkalinity during the T-OAE may have been counterbalanced by the accumulation of authigenic carbonate in epicontinental basins, which is a predicted consequence of higher organic matter supply ([Sun and Turchyn, 2014](#)). Indeed, authigenic carbonate beds and concretions are particularly common in T-OAE successions (e.g., [Howarth, 1962](#); [Bréhéret et al., 2004](#)); a conspicuous carbonate authigenic marker bed notably occurs immediately before the positive limb of the T-OAE CIE in UK (the ‘whale stones’; bed 35 of [Howarth, 1962](#); [Kemp et al., 2005](#)), SW Germany (‘Unterer Stein’; [Röhl et al., 2001](#)), S France (‘Leptolepis bed’, [Mailliot et al., 2009](#); [Harazim et al., 2013](#)) and in N Siberia ([Suan et al., 2011](#)), possibly representing humongous amounts of  $\text{CaCO}_3$ . In any case, the causes of the delayed recovery of carbonate accumulation after the T-OAE should be further scrutinized using micro-paleontological and geochemical data from sites located outside Europe as well as more sophisticated isotope models integrating realistic connections between the calcium, carbon and carbonate cycles.

### 5.5. Estimation of the amount and isotopic signature of excess atmospheric $\text{CO}_2$

The global warming pulses recorded for the PI-To and T-OAE intervals require the massive input of atmospheric  $\text{CO}_2$  in the form of volcanism degassing or methane hydrate dissociation. A first order approximation is that each mole of excess calcium added to ocean requires 0.5 mole of  $\text{CO}_2$  ([Payne et al., 2010](#)). Calcium discharge to the ocean of the modern largest rivers is derived for about one quarter from silicates weathering, which plays a role

in the atmospheric  $\text{CO}_2$  drawdown over long time scale ([Walker et al., 1981](#); [Gaillardet et al., 1999](#)). Accordingly, the amount of carbon added to the superficial reservoirs required to reproduce a 500% increase in continental runoff during 150 kyr approximated 40 000 GtC.

It is therefore possible to perform a simple mass balance equation (considering the events as instantaneous) to determine the  $\delta^{13}\text{C}$  composition required to explain the Toarcian CIEs. The mass balance equation is similar to that used in previous studies ([Dickens et al., 1995](#)):

$$M_f \times \delta^{13}\text{C}_f = M_i \times \delta^{13}\text{C}_i + M_p \times \delta^{13}\text{C}_p$$

with  $M_f = M_i + M_p$ , where  $M_f$  and  $M_i$  are the final and initial dissolved inorganic carbon (DIC) reservoir size,  $M_p$  the mass of carbon added during perturbations and  $\delta^{13}\text{C}_f$ ,  $\delta^{13}\text{C}_i$ ,  $\delta^{13}\text{C}_p$  the respective isotopic composition of carbon. The values of the different parameters and the results of calculation are presented in [Table 3](#).

According to these calculations, the  $\delta^{13}\text{C}$  of the carbon released at the onset of the PI-To and T-OAE vary from  $-11.4$  to  $-6.3\%$  and from  $-13.6$  to  $-8.2\%$ . These isotopic compositions are slightly lower than that commonly admitted for volcanism degassing ( $\sim -7\%$ ; [Hesselbo et al., 2007](#)) but still within the range of measured  $\delta^{13}\text{C}$  values of mantle xenoliths ([Deines, 2002](#)). These simple calculations suggest that the dissociation of the methane hydrates ( $\delta^{13}\text{C} \sim -60\%$ ) was likely not the foremost driver of the Toarcian CIEs. Nevertheless, an input from mixed source with a contribution from methane hydrates dissociation cannot be totally excluded, and may explain the abrupt shift toward negative  $\delta^{13}\text{C}$  values documented at the onset of the T-OAE excursion in many marine records ([Hesselbo et al., 2007](#); [Suan et al., 2008a](#)). It must be noted that above calculations, based on simplistic models, should await confirmation by more realistic models integrating fully coupled carbon and calcium cycles. Such models, together with higher-resolution  $\delta^{44/40}\text{Ca}$  records from different paleoceanographic settings, hold promise for better constraining the chain of events that led to the severe perturbations recorded in Pliensbachian–Toarcian strata.

## 6. Conclusion

This study reports calcium isotope data of well preserved brachiopod shells and bulk samples from the Peniche succession in Portugal (Pliensbachian–Toarcian transition GSSP). Our results reveal two marked negative excursions close to the PI-To transition and the T-OAE intervals that show a clear parallelism with previously published  $\delta^{13}\text{C}$  from bulk carbonate and that from the same brachiopods shells. These data are interpreted as reflecting supra-regional changes in the  $\delta^{44/40}\text{Ca}$  of seawater linked to global

increase of continental weathering and episodes of ocean acidification at the onset of each perturbation. Calcium cycle box modeling indicates that a relatively long-lived, 500% increase in continental weathering following pulses of massive carbon injection adequately reproduces the magnitude and shape of each excursion. This scenario is consistent with independent evidence of warming and enhanced nutrient input during both events, and accounts for the apparent synchronicity between the  $\delta^{44/40}\text{Ca}$  and  $\delta^{13}\text{C}$  excursions recorded at Peniche. Nevertheless, the peak of carbonate accumulation recorded by most NW European marine sites after the T–OAE occurs at least several hundreds of kyr after that predicted by calcium cycle box-models. Several factors may explain this mismatch, and further investigations are needed to address the mode and tempo of enhanced carbonate burial as a response of higher continental weathering during the Pl–To and T–OAE events. Finally, simple mass balance calculations suggest that the carbon release during each of these events involved >40000 Gt of C with an isotopic composition ranging from  $-13.6$  to  $-6.3\%$ . Although a small contribution of methane hydrates dissociation cannot be totally excluded, these results point to the repeated and massive degassing of  $\text{CO}_2$  from Karoo–Ferrar LIP as the main cause of the environmental perturbation recorded across the Pl–To and T–OAE intervals.

### Acknowledgements

We are grateful to P. Telouk for his assistance with calcium isotope analyses, S. Bodin for discussion about Moroccan sections and A. Lena for his help with sample purification. We acknowledge H.C. Jenkyns and an anonymous reviewer for their constructive comments that helped to improve the quality of the manuscript. This work was funded by the French INSU–CNRS program SYSTER to G.S.

### Appendix A. Supplementary material

Supplementary material related to this article can be found online at <http://dx.doi.org/10.1016/j.epsl.2014.11.028>.

### References

- Al-Suwaidi, A.H., Angelozzi, G.N., Baudin, F., Damborenea, S.E., Hesselbo, S.P., Jenkyns, H.C., Manceñido, M.O., Riccardi, A.C., 2010. First record of the Early Toarcian Oceanic Anoxic Event from the Southern Hemisphere, Neuquén Basin, Argentina. *J. Geol. Soc.* 167, 633–636. <http://dx.doi.org/10.1144/0016-76492010-025>.
- Auclair, A.-C., Joachimski, M.M., Lécuyer, C., 2003. Deciphering kinetic, metabolic and environmental controls on stable isotope fractionations between seawater and the shell of *Terebratalia transversa* (Brachiopoda). *Chem. Geol.* 202, 59–78. [http://dx.doi.org/10.1016/S0009-2541\(03\)00233-X](http://dx.doi.org/10.1016/S0009-2541(03)00233-X).
- Bailey, T.R., Rosenthal, Y., McArthur, J.M., van de Schootbrugge, B., Thirlwall, M.F., 2003. Paleooceanographic changes of the Late Pliensbachian–Early Toarcian interval: a possible link to the genesis of an Oceanic Anoxic Event. *Earth Planet. Sci. Lett.* 212, 307–320. [http://dx.doi.org/10.1016/S0012-821X\(03\)00278-4](http://dx.doi.org/10.1016/S0012-821X(03)00278-4).
- Bjerrum, C.J., Surlyk, F., Callomon, J.H., Slingerland, R.L., 2001. Numerical paleoceanographic study of the Early Jurassic Transcontinental Laurasian Seaway. *Paleoceanography* 16, 390–404. <http://dx.doi.org/10.1029/2000PA000512>.
- Blättler, C.L., Jenkyns, H.C., Reynard, L.M., Henderson, G.M., 2011. Significant increases in global weathering during Oceanic Anoxic Events 1a and 2 indicated by calcium isotopes. *Earth Planet. Sci. Lett.* 309, 77–88. <http://dx.doi.org/10.1016/j.epsl.2011.06.029>.
- Blättler, C.L., Henderson, G.M., Jenkyns, H.C., 2012. Explaining the Phanerozoic Ca isotope history of seawater. *Geology* 40, 843–846. <http://dx.doi.org/10.1130/G33191.1>.
- Boulila, S., Galbrun, B., Huret, E., Hinnov, L.A., Rouget, I., Gardin, S., Bartolini, A., 2014. Astronomical calibration of the Toarcian stage: implications for sequence stratigraphy and duration of the early Toarcian OAE. *Earth Planet. Sci. Lett.* 386, 98–111. <http://dx.doi.org/10.1016/j.epsl.2013.10.047>.
- Brand, U., Logan, A., Hiller, N., Richardson, J., 2003. Geochemistry of modern brachiopods: applications and implications for oceanography and paleoceanography. *Chem. Geol.* 198, 305–334. [http://dx.doi.org/10.1016/S0009-2541\(03\)00032-9](http://dx.doi.org/10.1016/S0009-2541(03)00032-9).
- Bréhéret, J.-G., Hanzo, M., El Albani, A., Iatzioura, A., 2004. Impact de la vie benthique sur la genèse de nodules calcaires dans les black shales. *C. R. Géosci.* 336, 1355–1362. <http://dx.doi.org/10.1016/j.crte.2004.09.002>.
- Carpenter, S.J., Lohmann, K.C., 1995.  $\delta^{18}\text{O}$  and  $\delta^{13}\text{C}$  values of modern brachiopod shells. *Geochim. Cosmochim. Acta* 59, 3749–3764. [http://dx.doi.org/10.1016/0016-7037\(95\)00291-7](http://dx.doi.org/10.1016/0016-7037(95)00291-7).
- Caruthers, A.H., Gröcke, D.R., Smith, P.L., 2011. The significance of an Early Jurassic (Toarcian) carbon-isotope excursion in Haida Gwaii (Queen Charlotte Islands), British Columbia, Canada. *Earth Planet. Sci. Lett.* 307, 19–26. <http://dx.doi.org/10.1016/j.epsl.2011.04.013>.
- Cecca, F., Macchioni, F., 2004. The two Early Toarcian (Early Jurassic) extinction events in ammonoids. *Lethaia* 37, 35–56. <http://dx.doi.org/10.1080/00241160310008257>.
- Cohen, A.S., Coe, A.L., Harding, S.M., Schwark, L., 2004. Osmium isotope evidence for the regulation of atmospheric  $\text{CO}_2$  by continental weathering. *Geology* 32, 157–160. <http://dx.doi.org/10.1130/G20158.1>.
- Cohen, A.S., Coe, A.L., Kemp, D.B., 2007. The Late Palaeocene–Early Eocene and Toarcian (Early Jurassic) carbon isotope excursions: a comparison of their time scales, associated environmental changes, causes and consequences. *J. Geol. Soc.* 164, 1093–1108. <http://dx.doi.org/10.1144/0016-76492006-123>.
- Coplen, T.B., Hoppfe, J.A., Böhlke, J.K., Peiser, H.S., Rieder, S.E., Krouse, H.R., Rosman, K.J.R., Ding, T., Vocke, J.R.D., Révész, K.M., Lamberty, A., Taylor, P., De Bièvre, P., 2002. Compilation of minimum and maximum isotope ratios of selected elements in naturally occurring terrestrial materials and reagents. U.S. Dept. of the Interior, U.S. Geological Survey.
- De LaRocha, C.L., DePaolo, D.J., 2000. Isotopic evidence for variations in the marine calcium cycle over the cenozoic. *Science* 289, 1176–1178. <http://dx.doi.org/10.1126/science.289.5482.1176>.
- Deines, P., 2002. The carbon isotope geochemistry of mantle xenoliths. *Earth-Sci. Rev.* 58, 247–278.
- DePaolo, D.J., 2004. Calcium isotopic variations produced by biological, kinetic, radiogenic and nucleosynthetic processes. *Rev. Mineral. Geochem.* 55, 255–288. <http://dx.doi.org/10.2138/gsrng.55.1.255>.
- Dera, G., Pellenard, P., Neige, P., Deconinck, J.-F., Pucéat, E., Dommergues, J.-L., 2009. Distribution of clay minerals in Early Jurassic Peritethyan seas: palaeoclimatic significance inferred from multiproxy comparisons. *Palaeogeogr. Palaeoclimatol. Palaeoecol.* 271, 39–51. <http://dx.doi.org/10.1016/j.palaeo.2008.09.010>.
- Dickens, G.R., O’Neil, J.R., Rea, D.K., Owen, R.M., 1995. Dissociation of oceanic methane hydrate as a cause of the carbon isotope excursion at the end of the Paleocene. *Paleoceanography* 10, 965–971. <http://dx.doi.org/10.1029/95PA02087>.
- Dickson, J.A.D., 2004. Echinoderm skeletal preservation: calcite–aragonite seas and the Mg/Ca ratio of phanerozoic oceans. *J. Sediment. Res.* 74, 355–365.
- Dromart, G., Allemand, P., Garcia, J.-P., Robin, C., 1996. Variation cyclique de la production carbonatée au Jurassique le long d’un transect Bourgogne–Ardeche, Est-France. *Bull. Soc. Géol. Fr.* 167, 423–433.
- Duarte, L.V., Wright, V.P., Fernandez-Lopez, S., Elmi, S., Krautter, M., Azerêdo, A., Henriques, M.H., Rodrigues, R., Perilli, N., 2004. Early Jurassic carbonate evolution in the Lusitanian Basin: facies, sequence stratigraphy and cyclicity. In: Duarte, L.V., Henriques, M.H. (Eds.), Carboniferous and Jurassic Carbonate Platforms of Iberia. 23rd IAS Meeting of Sedimentology.
- Elmi, S., 2006. Pliensbachian/Toarcian boundary: the proposed GSSP, Peniche (Portugal). *Vol. Jurassica* 4 (4), 5–16.
- Fantle, M.S., DePaolo, D.J., 2005. Variations in the marine Ca cycle over the past 20 million years. *Earth Planet. Sci. Lett.* 237, 102–117. <http://dx.doi.org/10.1016/j.epsl.2005.06.024>.
- Fantle, M.S., Higgins, J., 2014. The effects of diagenesis and dolomitization on Ca and Mg isotopes in marine platform carbonates: implications for the geochemical cycles of Ca and Mg. *Geochim. Cosmochim. Acta* 142, 458–481.
- Farkaš, J., Buhl, D., Blenkinsop, J., Veizer, J., 2007a. Evolution of the oceanic calcium cycle during the late Mesozoic: evidence from  $\delta^{44/40}\text{Ca}$  of marine skeletal carbonates. *Earth Planet. Sci. Lett.* 253, 96–111. <http://dx.doi.org/10.1016/j.epsl.2006.10.015>.
- Farkaš, J., Böhm, F., Wallmann, K., Blenkinsop, J., Eisenhauer, A., van Geldern, R., Munnecke, A., Voigt, S., Veizer, J., 2007b. Calcium isotope record of Phanerozoic oceans: implications for chemical evolution of seawater and its causative mechanisms. *Geochim. Cosmochim. Acta* 71, 5117–5134. <http://dx.doi.org/10.1016/j.gca.2007.09.004>.
- Gaillardet, J., Dupré, B., Louvat, P., Allègre, C.J., 1999. Global silicate weathering and  $\text{CO}_2$  consumption rates deduced from the chemistry of large rivers. *Chem. Geol.* 159, 3–30. [http://dx.doi.org/10.1016/S0009-2541\(99\)00031-5](http://dx.doi.org/10.1016/S0009-2541(99)00031-5).
- Gómez, J.J., Goy, A., 2011. Warming-driven mass extinction in the Early Toarcian (Early Jurassic) of northern and central Spain. Correlation with other time-equivalent European sections. *Palaeogeogr. Palaeoclimatol. Palaeoecol.* 306, 176–195. <http://dx.doi.org/10.1016/j.palaeo.2011.04.018>.
- Gómez, J.J., Goy, A., Canales, M.L., 2008. Seawater temperature and carbon isotope variations in belemnites linked to mass extinction during the Toarcian (Early Jurassic) in Central and Northern Spain. Comparison with other European sections. *Palaeogeogr. Palaeoclimatol. Palaeoecol.* 258, 28–58. <http://dx.doi.org/10.1016/j.palaeo.2007.11.005>.

- Gussone, N., Böhm, F., Eisenhauer, A., Dietzel, M., Heuser, A., Teichert, B.M.A., Reitner, J., Wörheide, G., Dullo, W.-C., 2005. Calcium isotope fractionation in calcite and aragonite. *Geochim. Cosmochim. Acta* 69, 4485–4494. <http://dx.doi.org/10.1016/j.gca.2005.06.003>.
- Harazim, D., Van De Schootbrugge, B., Sorichter, K., Fiebig, J., Weug, A., Suan, G., Oschmann, W., 2013. Spatial variability of watermass conditions within the European Epicontinental Seaway during the Early Jurassic (Pliensbachian–Toarcian). *Sedimentology* 60, 359–390. <http://dx.doi.org/10.1111/j.1365-3091.2012.01344.x>.
- Hermoso, M., Minoletti, F., Le Gallonnet, L., Jenkyns, H.C., Hesselbo, S.P., Rickaby, R.E.M., Renard, M., de Rafelis, M., Emmanuel, L., 2009. Global and local forcing of Early Toarcian seawater chemistry: a comparative study of different paleoceanographic settings (Paris and Lusitanian basins). *Paleoceanography* 24.
- Hesselbo, S.P., Gröcke, D.R., Jenkyns, H.C., Bjerrum, C.J., Farrimond, P., Morgans Bell, H.S., Green, O.R., 2000. Massive dissociation of gas hydrate during a Jurassic oceanic anoxic event. *Nature* 406, 392–395. <http://dx.doi.org/10.1038/35019044>.
- Hesselbo, S.P., Jenkyns, H.C., Duarte, L.V., Oliveira, L.C.V., 2007. Carbon-isotope record of the Early Jurassic (Toarcian) Oceanic Anoxic Event from fossil wood and marine carbonate (Lusitanian Basin, Portugal). *Earth Planet. Sci. Lett.* 253, 455–470. <http://dx.doi.org/10.1016/j.epsl.2006.11.009>.
- Heuser, A., Eisenhauer, A., 2008. The calcium isotope composition ( $\delta^{44/40}\text{Ca}$ ) of NIST SRM 915b and NIST SRM 1486. *Geostand. Geoanal. Res.* 32, 311–315. <http://dx.doi.org/10.1111/j.1751-908X.2008.00877.x>.
- Heuser, A., Eisenhauer, A., Böhm, F., Wallmann, K., Gussone, N., Pearson, P.N., Nägler, T.F., Dullo, W.-C., 2005. Calcium isotope ( $\delta^{44/40}\text{Ca}$ ) variations of Neogene planktonic foraminifera. *Paleoceanography* 20, PA2013. <http://dx.doi.org/10.1029/2004PA001048>.
- Hinojosa, J.L., Brown, S.T., Chen, J., DePaolo, D.J., Paytan, A., Shen, S., Payne, J.L., 2012. Evidence for end-Permian oceanic anoxification from calcium isotopes in biogenic apatite. *Geology* 40, 743–746. <http://dx.doi.org/10.1130/G33048.1>.
- Hippler, D., Schmitt, A.-D., Gussone, N., Heuser, A., Stille, P., Eisenhauer, A., Nägler, T.F., 2003. Calcium isotopic composition of various reference materials and Seawater. *Geostand. Newsl.* 27, 13–19. <http://dx.doi.org/10.1111/j.1751-908X.2003.tb00709.x>.
- Holmden, C., 2009. Ca isotope study of Ordovician dolomite, limestone, and anhydrite in the Williston Basin: implications for subsurface dolomitization and local Ca cycling. *Chem. Geol.* 268, 180–188. <http://dx.doi.org/10.1016/j.chemgeo.2009.08.009>.
- Hönisch, B., Ridgwell, A., Schmidt, D.N., Thomas, E., Gibbs, S.J., Sluijs, A., Zeebe, R., Kump, L., Martindale, R.C., Greene, S.E., Kiessling, W., Ries, J., Zachos, J.C., Royer, D.L., Barker, S., Marchitto, T.M., Moyer, R., Pelejero, C., Ziveri, P., Foster, G.L., Williams, B., 2012. The geological record of ocean acidification. *Science* 335, 1058–1063. <http://dx.doi.org/10.1126/science.1208277>.
- Howard, A.S., 1985. Lithostratigraphy of the Staithes Sandstone and Cleveland Ironstone formations (Lower Jurassic) of north-east Yorkshire. *Proc. of the Yorks. Geol. and Polytech. Soc.* 45, 261–275. <http://dx.doi.org/10.1144/pygs.45.4.261>.
- Howarth, M.K., 1962. The Jet Rock Series and the Alum Shale Series of the Yorkshire Coast. *Proc. of the Yorks. Geol. and Polytech. Soc.* 33, 381–422. <http://dx.doi.org/10.1144/pygs.33.4.381>.
- Huang, C., Hesselbo, S.P., 2013. Pacing of the Toarcian Oceanic Anoxic Event (Early Jurassic) from astronomical correlation of marine sections. *Gondwana Res.* <http://dx.doi.org/10.1016/j.jgr.2013.06.023>.
- Huber, B.T., Macleod, K.G., Wing, S.L., 2000. *Warm Climates in Earth History*. Cambridge University Press.
- Izumi, K., Miyaji, T., Tanabe, K., 2012. Early Toarcian (Early Jurassic) oceanic anoxic event recorded in the shelf deposits in the northwestern Panthalassa: evidence from the Nishinakayama formation in the Toyora area, west Japan. *Paleoogeogr. Palaeoclimatol. Palaeoecol.* 315–316, 100–108. <http://dx.doi.org/10.1016/j.palaeo.2011.11.016>.
- Jenkyns, H.C., 1988. The early Toarcian (Jurassic) anoxic event: stratigraphic, sedimentary and geochemical evidence. *Am. J. Sci.* 288, 101–151. <http://dx.doi.org/10.2475/ajs.288.2.101>.
- Jenkyns, H.C., 2010. Geochemistry of oceanic anoxic events. *Geochim. Geophys. Geosyst.* 11, Q03004. <http://dx.doi.org/10.1029/2009GC002788>.
- Jenkyns, H.C., Gröcke, D.R., Hesselbo, S.P., 2001. Nitrogen isotope evidence for water mass denitrification during the Early Toarcian (Jurassic) oceanic anoxic event. *Paleoceanography* 16, 593–603. <http://dx.doi.org/10.1029/2000PA000558>.
- Kemp, D.B., Coe, A.L., Cohen, A.S., Schwark, L., 2005. Astronomical pacing of methane release in the Early Jurassic period. *Nature* 437, 396–399. <http://dx.doi.org/10.1038/nature04037>.
- Kemp, D.B., Coe, A.L., Cohen, A.S., Weedon, G.P., 2011. Astronomical forcing and chronology of the early Toarcian (Early Jurassic) oceanic anoxic event in Yorkshire, UK. *Paleoceanography* 26, PA4210. <http://dx.doi.org/10.1029/2011PA002122>.
- Krencker, F.-N., Bodin, S., Suan, G., Kabiri, L., Immenhauser, A., 2013. Assessing the duration and possible causes of the earliest Toarcian carbon isotopic excursion. In: EGU General Assembly Conference Abstracts. Presented at the EGU General Assembly Conference Abstracts, p. 4970.
- Kump, L., Bralower, T., Ridgwell, A., 2009. Ocean acidification in deep time. *Oceanography* 22, 94–107. <http://dx.doi.org/10.5670/oceanog.2009.100>.
- Küspert, W., 1982. Environmental changes during oil shale deposition as deduced from stable isotope ratios. In: Einsele, P.D.G., Seilacher, P.D.A. (Eds.), *Cyclic and Event Stratification*. Springer, Berlin, Heidelberg, pp. 482–501.
- Littler, K., Hesselbo, S.P., Jenkyns, H.C., 2010. A carbon-isotope perturbation at the Pliensbachian–Toarcian boundary: evidence from the Lias Group, NE England. *Geol. Mag.* 147, 181–192. <http://dx.doi.org/10.1017/S0016756809990458>.
- Mailliot, S., Mattioli, E., Bartolini, A., Baudin, F., Pittet, B., Guex, J., 2009. Late Pliensbachian–Early Toarcian (Early Jurassic) environmental changes in an epicontinental basin of NW Europe (Causse area, central France): a micropaleontological and geochemical approach. *Paleoogeogr. Palaeoclimatol. Palaeoecol.* 273, 346–364. <http://dx.doi.org/10.1016/j.palaeo.2008.05.014>.
- Mattioli, E., Pittet, B., 2002. Contribution of calcareous nannoplankton to carbonate deposition: a new approach applied to the Lower Jurassic of central Italy. *Mar. Micropaleontol.* 45, 175–190. [http://dx.doi.org/10.1016/S0377-8398\(02\)00039-7](http://dx.doi.org/10.1016/S0377-8398(02)00039-7).
- Mattioli, E., Pittet, B., Palliani, R., Röhl, H.-J., Schmid-Röhl, A., Moretini, E., 2004. Phytoplankton evidence for the timing and correlation of paleoceanographical changes during the early Toarcian oceanic anoxic event (Early Jurassic). *J. Geol. Soc.* 161, 685–693. <http://dx.doi.org/10.1144/0016-764903-074>.
- Mattioli, E., Pittet, B., Suan, G., Mailliot, S., 2008. Calcareous nannoplankton changes across the early Toarcian oceanic anoxic event in the western Tethys. *Paleoceanography* 23, PA3208. <http://dx.doi.org/10.1029/2007PA001435>.
- Mattioli, E., Pittet, B., Petitpierre, L., Mailliot, S., 2009. Dramatic decrease of pelagic carbonate production by nannoplankton across the Early Toarcian anoxic event (T–OAE). *Glob. Planet. Change* 65, 134–145. <http://dx.doi.org/10.1016/j.jglapla.2008.10.018>.
- McArthur, J.M., Donovan, D.T., Thirlwall, M.F., Fouke, B.W., Matthey, D., 2000. Strontium isotope profile of the early Toarcian (Jurassic) oceanic anoxic event, the duration of ammonite biozones, and belemnite palaeotemperatures. *Earth Planet. Sci. Lett.* 179, 269–285. [http://dx.doi.org/10.1016/S0012-821X\(00\)00111-4](http://dx.doi.org/10.1016/S0012-821X(00)00111-4).
- McArthur, J.M., Algeo, T.J., van de Schootbrugge, B., Li, Q., Howarth, R.J., 2008. Basinal restriction, black shales, Re–Os dating, and the Early Toarcian (Jurassic) oceanic anoxic event. *Paleoceanography* 23, PA4217. <http://dx.doi.org/10.1029/2008PA001607>.
- McElwain, J.C., Wade-Murphy, J., Hesselbo, S.P., 2005. Changes in carbon dioxide during an oceanic anoxic event linked to intrusion into Gondwana coals. *Nature* 435, 479–482. <http://dx.doi.org/10.1038/nature03618>.
- Morard, A., Guex, J., Bartolini, A., Moretini, E., de Wever, P., 2003. A new scenario for the Domesian–Toarcian transition. *Bull. Soc. Géol. Fr.* 174, 351–356. <http://dx.doi.org/10.2113/174.4.351>.
- Morgan, J.L.L., Gordon, G.W., Arrua, R.C., Skulan, J.L., Anbar, A.D., Bullen, T.D., 2011. High-precision measurement of variations in calcium isotope ratios in urine by multiple collector inductively coupled plasma mass spectrometry. *Anal. Chem.* 83, 6956–6962. <http://dx.doi.org/10.1021/ac200361t>.
- Palliani, R.B., Riding, J.B., 2003. Biostratigraphy, provincialism and evolution of European early Jurassic (Pliensbachian to early Toarcian) dinoflagellate cysts. *Paleontology* 27, 179–214. <http://dx.doi.org/10.1080/01916122.2003.9989586>.
- Parkinson, D., Curry, G.B., Cusack, M., Fallick, A.E., 2005. Shell structure, patterns and trends of oxygen and carbon stable isotopes in modern brachiopod shells. *Chem. Geol.* 219, 193–235. <http://dx.doi.org/10.1016/j.chemgeo.2005.02.002>.
- Payne, J.L., Turchyn, A.V., Paytan, A., DePaolo, D.J., Lehrmann, D.J., Yu, M., Wei, J., 2010. Calcium isotope constraints on the end-Permian mass extinction. *Proc. Natl. Acad. Sci. USA* 107, 8543–8548. <http://dx.doi.org/10.1073/pnas.0914065107>.
- Pittet, B., Suan, G., Lenoir, F., Duarte, L.V., Mattioli, E., 2014. Carbon isotope evidence for sedimentary discontinuities in the lower Toarcian of the Lusitanian Basin (Portugal): sea level change at the onset of the Oceanic Anoxic Event. *Sediment. Geol.* 303, 1–14. <http://dx.doi.org/10.1016/j.sedgeo.2014.01.001>.
- Reynard, L.M., Henderson, G.M., Hedges, R.E.M., 2010. Calcium isotope ratios in animal and human bone. *Geochim. Cosmochim. Acta* 74, 3735–3750.
- Ridgwell, A., 2005. A Mid Mesozoic Revolution in the regulation of ocean chemistry. *Mar. Geol.* 217, 339–357.
- Röhl, H.-J., Schmid-Röhl, A., Oschmann, W., Frimmel, A., Schwark, L., 2001. The Posidonia Shale (Lower Toarcian) of SW-Germany: an oxygen-depleted ecosystem controlled by sea level and palaeoclimate. *Paleoogeogr. Palaeoclimatol. Palaeoecol.* 165, 27–52. [http://dx.doi.org/10.1016/S0012-821X\(00\)00152-8](http://dx.doi.org/10.1016/S0012-821X(00)00152-8).
- Rustad, J.R., Casey, W.H., Yin, Q.-Z., Bylaska, E.J., Felmy, A.R., Bogatko, S.A., Jackson, V.E., Dixon, D.A., 2010. Isotopic fractionation of  $\text{Mg}^{2+}$  (aq),  $\text{Ca}^{2+}$  (aq), and  $\text{Fe}^{2+}$  (aq) with carbonate minerals. *Geochim. Cosmochim. Acta* 74, 6301–6323.
- Sabatino, N., Neri, R., Bellanca, A., Jenkyns, H.C., Baudin, F., Parisi, G., Masetti, D., 2009. Carbon-isotope records of the Early Jurassic (Toarcian) oceanic anoxic event from the Valdorbia (Umbria–Marche Apennines) and Monte Mangart (Julian Alps) sections: paleoceanographic and stratigraphic implications. *Sedimentology* 56, 1307–1328. <http://dx.doi.org/10.1111/j.1365-3091.2008.01035.x>.
- Sandberg, P.A., 1983. An oscillating trend in Phanerozoic non-skeletal carbonate mineralogy. *Nature* 305, 19–22.
- Schlager, W., James, N.P., 1978. Low-magnesian calcite limestones forming at the deep-sea floor, Tongue of the Ocean, Bahamas. *Sedimentology* 25, 675–702.
- Schmitt, A.-D., Chabaux, F., Stille, P., 2003. The calcium riverine and hydrothermal isotopic fluxes and the oceanic calcium mass balance. *Earth Planet. Sci. Lett.* 213, 503–518. [http://dx.doi.org/10.1016/S0012-821X\(03\)00341-8](http://dx.doi.org/10.1016/S0012-821X(03)00341-8).

- Stanley, S.M., Hardie, L.A., 1998. Secular oscillations in the carbonate mineralogy of reef-building and sediment-producing organisms driven by tectonically forced shifts in seawater chemistry. *Palaeogeogr. Palaeoclimatol. Palaeoecol.* 144, 3–19.
- Suan, G., Mattioli, E., Pittet, B., Mailliot, S., Lécuyer, C., 2008a. Evidence for major environmental perturbation prior to and during the Toarcian (Early Jurassic) oceanic anoxic event from the Lusitanian Basin, Portugal. *Paleoceanography* 23, PA1202. <http://dx.doi.org/10.1029/2007PA001459>.
- Suan, G., Pittet, B., Bour, I., Mattioli, E., Duarte, L.V., Mailliot, S., 2008b. Duration of the Early Toarcian carbon isotope excursion deduced from spectral analysis: consequence for its possible causes. *Earth Planet. Sci. Lett.* 267, 666–679. <http://dx.doi.org/10.1016/j.epsl.2007.12.017>.
- Suan, G., Mattioli, E., Pittet, B., Lécuyer, C., Suchéras-Marx, B., Duarte, L.V., Philippe, M., Reggiani, L., Martineau, F., 2010. Secular environmental precursors to Early Toarcian (Jurassic) extreme climate changes. *Earth Planet. Sci. Lett.* 290, 448–458. <http://dx.doi.org/10.1016/j.epsl.2009.12.047>.
- Suan, G., Nikitenko, B.L., Rogov, M.A., Baudin, F., Spangenberg, J.E., Knyazev, V.G., Glinskikh, L.A., Goryacheva, A.A., Adatte, T., Riding, J.B., Föllmi, K.B., Pittet, B., Mattioli, E., Lécuyer, C., 2011. Polar record of Early Jurassic massive carbon injection. *Earth Planet. Sci. Lett.* 312, 102–113. <http://dx.doi.org/10.1016/j.epsl.2011.09.050>.
- Sun, X., Turchyn, A.V., 2014. Significant contribution of authigenic carbonate to marine carbon burial. *Nat. Geosci.* 7, 201–204. <http://dx.doi.org/10.1038/ngeo2070>.
- Svensen, H., Planke, S., Chevallerier, L., Malthes-Sørenssen, A., Corfu, F., Jamtveit, B., 2007. Hydrothermal venting of greenhouse gases triggering Early Jurassic global warming. *Earth Planet. Sci. Lett.* 256, 554–566. <http://dx.doi.org/10.1016/j.epsl.2007.02.013>.
- Tacail, T., Albalat, E., Télouk, P., Balter, V., 2014. A simplified protocol for measurement of Ca isotopes in biological samples. *J. Anal. At. Spectrom.* 29, 529–535. <http://dx.doi.org/10.1039/C3JA50337B>.
- Trecalli, A., Spangenberg, J., Adatte, T., Föllmi, K.B., Parente, M., 2012. Carbonate platform evidence of ocean acidification at the onset of the early Toarcian oceanic anoxic event. *Earth Planet. Sci. Lett.* 357–358, 214–225. <http://dx.doi.org/10.1016/j.epsl.2012.09.043>.
- van Breugel, Y., Baas, M., Schouten, S., Mattioli, E., Sinninghe Damsté, J.S., 2006. Isorenieratane record in black shales from the Paris Basin, France: constraints on recycling of respired CO<sub>2</sub> as a mechanism for negative carbon isotope shifts during the Toarcian oceanic anoxic event. *Paleoceanography* 21, PA4220. <http://dx.doi.org/10.1029/2006PA001305>.
- van de Schootbrugge, B., Bailey, T.R., Rosenthal, Y., Katz, M.E., Wright, J.D., Miller, K.G., Feist-Burkhardt, S., Falkowski, P.G., 2005. Early Jurassic climate change and the radiation of organic-walled phytoplankton in the Tethys Ocean. *Paleobiology* 31, 73–97. [http://dx.doi.org/10.1666/0094-8373\(2005\)031<0073:EJCCAT>2.0.CO;2](http://dx.doi.org/10.1666/0094-8373(2005)031<0073:EJCCAT>2.0.CO;2).
- Von Allmen, K., Nägler, T.F., Pettke, T., Hippler, D., Griesshaber, E., Logan, A., Eisenhauer, A., Samankassou, E., 2010. Stable isotope profiles (Ca, O, C) through modern brachiopod shells of *T. septentrionalis* and *G. vitreus*: implications for calcium isotope paleo-ocean chemistry. *Chem. Geol.* 269, 210–219. <http://dx.doi.org/10.1016/j.chemgeo.2009.09.019>.
- Walker, J.C.G., Hays, P.B., Kasting, J.F., 1981. A negative feedback mechanism for the long-term stabilization of Earth's surface temperature. *J. Geophys. Res., Oceans* 86, 9776–9782. <http://dx.doi.org/10.1029/JC086iC10p09776>.
- Waltham, D., Gröcke, D.R., 2006. Non-uniqueness and interpretation of the seawater <sup>87</sup>Sr/<sup>86</sup>Sr curve. *Geochim. Cosmochim. Acta* 70, 384–394. <http://dx.doi.org/10.1016/j.gca.2005.09.014>.
- Wignall, P.B., 1991. Model for transgressive black shales? *Geology* 19, 167–170. [http://dx.doi.org/10.1130/0091-7613\(1991\)019<0167:MFTBS>2.3.CO;2](http://dx.doi.org/10.1130/0091-7613(1991)019<0167:MFTBS>2.3.CO;2).
- Wignall, P.B., Bond, D.P.C., 2008. The end-Triassic and Early Jurassic mass extinction records in the British Isles. *Proc. Geol. Assoc.* 119, 73–84. [http://dx.doi.org/10.1016/S0016-7878\(08\)80259-3](http://dx.doi.org/10.1016/S0016-7878(08)80259-3).